Atmos. Chem. Phys., 25, 12069–12086, 2025 https://doi.org/10.5194/acp-25-12069-2025 © Author(s) 2025. This work is distributed under the Creative Commons Attribution 4.0 License.





Anthropogenic and natural causes for the interannual variation of PM_{2.5} in East Asia during summer monsoon periods from 2008 to 2018

Danyang Ma¹, Min Xie¹, Huan He¹, Tijian Wang², Mengzhu Xi¹, Lingyun Feng¹, Shuxian Zhang¹, and Shitong Chen¹

¹School of Environment, Nanjing Normal University, Nanjing 210023, China ²School of Atmospheric Sciences, Nanjing University, Nanjing 210023, China

Correspondence: Min Xie (minxie@njnu.edu.cn) and Tijian Wang (tjwang@nju.edu.cn)

Received: 2 January 2025 – Discussion started: 14 April 2025 Revised: 4 July 2025 – Accepted: 17 July 2025 – Published: 6 October 2025

Abstract. There was a significant difference in near-surface $PM_{2.5}$ across China after the implementation of the Clean Air Action Plan in 2013. This study used the regional climate-chemistry-ecosystem coupled model RegCM-Chem-YIBs to investigate interannual variations in $PM_{2.5}$ across East Asia from 2008 to 2018. The drivers of $PM_{2.5}$ variability were examined from anthropogenic and natural perspectives. Compared to 2008, $PM_{2.5}$ showed little variation during the pre-governance (PreG) period (2009–2013). However, during the postgovernance (PostG) period (2014–2018), a substantial decline in $PM_{2.5}$ was simulated, particularly in the North China Plain ($-36.76\,\mu\mathrm{g}\,\mathrm{m}^{-3}$) and the Sichuan Basin ($-33.96\,\mu\mathrm{g}\,\mathrm{m}^{-3}$). Anthropogenic pollutant emissions were the primary drivers of $PM_{2.5}$ reductions, contributing -10.39 to $-3.82\,\mu\mathrm{g}\,\mathrm{m}^{-3}$ in the PreG period and -33.86 to $-8.45\,\mu\mathrm{g}\,\mathrm{m}^{-3}$ in the PostG period. The influence of meteorological conditions on $PM_{2.5}$ during the PreG period (-6.31 to $2.32\,\mu\mathrm{g}\,\mathrm{m}^{-3}$) was comparable to that of anthropogenic pollutant emissions. Additionally, in the vegetation-rich region, the impact of CO_2 emission changes on $PM_{2.5}$ was comparable to that of anthropogenic pollutant emissions. Our study comprehensively examined the drivers of $PM_{2.5}$ concentration changes from 2008 to 2018. We highlight a significant intensification in the contribution of anthropogenic pollutant emissions and reveal that, in regions characterized by dense vegetation, changes in CO_2 concentrations exert a pronounced impact on $PM_{2.5}$ variations.

1 Introduction

 $PM_{2.5}$ refers to fine particulate matter with an aerodynamic diameter less than or equal to $2.5\,\mu m$ (Chen et al., 2018). Its sources include industrial emissions, vehicular exhaust, biomass burning, and secondary formation from atmospheric gases (Wu et al., 2020). Major chemical components of $PM_{2.5}$ include sulfates, nitrates, ammonium salts, organic carbon, elemental carbon, and heavy metals (van Donkelaar et al., 2019; Li et al., 2017a). $PM_{2.5}$ is one of the primary atmospheric pollutants in China (Fontes et al., 2017), posing significant risks to human respiratory health (Feng et al., 2016; Xing et al., 2016). Long-term exposure to $PM_{2.5}$ can lead to respiratory diseases such as chronic bronchitis, em-

physema, and asthma (Kim et al., 2015; Pui et al., 2014; Xing et al., 2016). Additionally, $PM_{2.5}$ is critical as a short-lived species influencing atmospheric radiation processes (Hu et al., 2017). It affects the radiative energy balance of the Earth–atmosphere system by scattering or reflecting solar radiation (direct effect) (Wu et al., 2021) and altering cloud microphysical properties (indirect effect) (Wang et al., 2018a; Wu et al., 2021).

With China's rapid economic development, widespread $PM_{2.5}$ pollution became prevalent across the country in the early 21st century (Ma et al., 2016). In the most severely polluted urban areas, the annual average $PM_{2.5}$ concentration exceeded 100 μ g m⁻³ (van Donkelaar et al., 2010). From 2000 to 2008, the national average $PM_{2.5}$ concentration in

China was $49.4 \pm 14.2 \,\mu g \, m^{-3}$. In eastern China, the average concentration was $55.4 \pm 16.1 \,\mu g \, m^{-3}$, while the Beijing–Tianjin–Hebei region experienced average levels as high as $62.1 \pm 22.5 \,\mu g \, m^{-3}$. The Yangtze River Delta (YRD) saw an average concentration of $63.0 \pm 11.1 \,\mu g \, m^{-3}$, the Pearl River Delta (PRD) recorded an average of $52.4 \pm 5.8 \,\mu g \, m^{-3}$, and the Sichuan Basin averaged $61.6 \pm 13.4 \,\mu g \, m^{-3}$ (Wei et al., 2021). To mitigate the severe PM_{2.5} pollution, China implemented the Clean Air Action Plan in 2013 (Li et al., 2019). This policy led to a significant nationwide decrease in PM_{2.5} concentrations (Zhang et al., 2019), and there has been a notable improvement in air quality since that date (Vu et al., 2019; Li et al., 2018).

The variation in $PM_{2.5}$ concentrations is influenced by three key factors: anthropogenic pollutant emissions, meteorological conditions (Xiao et al., 2021), and carbon dioxide (CO₂) changes. Anthropogenic pollutant emissions encompass industrial production, transportation, and energy consumption (An et al., 2019), which release amounts of primary $PM_{2.5}$, as well as the precursors of secondary $PM_{2.5}$ such as volatile organic compounds (Kurokawa and Ohara, 2020) and nitrogen oxides (Wu et al., 2020; Zheng et al., 2021b; Kurokawa and Ohara, 2020). Consequently, reducing these emissions is essential for mitigating $PM_{2.5}$ concentrations, as they directly contribute to both the formation and persistence of particulate pollution (Zheng et al., 2018; Zhang et al., 2019).

Meteorological conditions play a significant role in influencing near-surface PM_{2.5} concentrations (Chen et al., 2020b; Xiao et al., 2021). Elevated temperatures can accelerate atmospheric chemical reactions (Mousavinezhad et al., 2021), including oxidation and photochemical processes, thereby promoting the formation of PM_{2.5} (Zhong et al., 2018). In addition, moderate increases in temperature can significantly enhance the emissions of biogenic volatile organic compounds (BVOCs) by stimulating the activity of the synthase enzyme. However, when temperatures exceed the physiological tolerance threshold of plants, decreased enzyme activity or metabolic disruption may suppress emissions (Lindwall et al., 2016; Kleist et al., 2012). Therefore, temperature changes can influence atmospheric PM_{2.5} concentrations by modulating the emissions of BVOCs. Precipitation aids in removing particulate matter from the atmosphere through wet deposition (Zhang et al., 2013), effectively reducing PM_{2.5} pollution levels (Wu et al., 2018). Additionally, wind speed and direction are crucial factors in the transport and dispersion of particulate matter (Li et al., 2017b). Higher wind speeds facilitate the dispersion of particulate matter over a wider area, reducing its local accumulation and mitigating air pollution in specific regions (Li et al., 2017b; Zhang et al., 2018). The increase in planetary boundary layer height (PBLH) strengthens atmospheric upward motion (Ait-Chaalal et al., 2016), thereby reducing near-surface PM_{2.5} concentrations (Pan et al., 2019).

Changes in CO₂ concentrations can influence PM_{2.5} pollution levels through several mechanisms. Elevated CO2 concentrations impact the atmospheric radiation balance, altering the distribution and intensity of precipitation (Cao et al., 2012), which directly affects PM_{2.5} concentrations by influencing wet deposition rates (Zhang et al., 2022). Additionally, changes in CO₂ concentrations can affect vegetation photosynthesis and growth, which alter the emissions of BVOCs that can participate in atmospheric chemical reactions to form secondary organic aerosols and thereby impact atmospheric PM_{2.5} concentrations (Sun et al., 2013, 2012). It is worth noting that elevated CO₂ concentrations may also directly inhibit BVOC emissions by reducing the activity of BVOC synthase enzymes (Heald et al., 2009; Pegoraro et al., 2004). Therefore, the impact of increased CO₂ on vegetation BVOC emissions can be either positive or negative, depending primarily on the relative strength of the inhibitory effect from enzyme suppression versus the stimulatory effect from enhanced photosynthesis (Sun et al., 2012). Isoprene is the most abundant species among BVOCs, so changes in CO2 concentrations can indirectly affect near-surface PM_{2.5} concentrations by influencing isoprene emissions from vegetation (Sun et al., 2013; Lin et al., 2013; Kramer et al., 2016).

Numerous studies have used statistical models and numerical simulations to investigate the impacts of meteorological conditions and anthropogenic pollutant emissions on PM_{2.5} concentration changes in China. The results consistently indicate that changes in anthropogenic pollutant emissions are the primary driver of PM_{2.5} variation. Zhang et al. (2019), using the WRF-CMAQ model at the national scale, found that meteorological conditions accounted for only 9 % of the total decline in PM_{2.5} concentrations during 2013-2017 in China, suggesting that emission reductions were the dominant factor. Similarly, based on a multiple linear regression model, Chen et al. (2020a) reported that anthropogenic pollutant emission reductions contributed 73 %, 87 %, and 84 % to the PM_{2.5} decline in the North China Plain, Yangtze River Delta, and PRD, respectively, while the contribution of meteorological conditions ranged from 10 % to 26 %. Cheng et al. (2019), also employing the WRF-CMAQ model, found that the decrease in PM_{2.5} concentrations in Beijing over the same period was mainly attributable to local (65.4%) and regional (22.5%) emission reductions, with meteorological conditions accounting for only 12.1 %.

Current research primarily emphasizes the impact of anthropogenic pollutant emissions (Zheng et al., 2018) and meteorological changes on $PM_{2.5}$ concentrations (Zhang et al., 2019; Zhai et al., 2019), while the potential influence of CO_2 concentration changes on $PM_{2.5}$ pollution levels remains largely underexplored. Additionally, following the implementation of the Clean Air Action Plan in 2013, significant decreases in $PM_{2.5}$ concentrations were observed in China. Concurrently, CO_2 levels continued to rise (Xu et al., 2022), with the influence of CO_2 on $PM_{2.5}$ strengthening annually. Therefore, it is essential to analyze the evolution of

PM_{2.5} concentrations from 2008 to 2018 in detail, and attribute changes in PM_{2.5} levels to every factor, such as anthropogenic pollutant emissions, meteorological conditions, and CO₂ variations.

2 Methods and data

2.1 Model description

In this study, we employed the coupled regional climatechemistry-ecology model RegCM-Chem-YIBs (Xie et al., 2019, 2024). The RegCM-Chem component simulates key meteorological variables, including temperature, humidity, precipitation, and radiation, along with atmospheric pollutants including ozone and particulate matter (Shalaby et al., 2012). The YIBs (Yale Interactive terrestrial Biosphere) model focuses on simulating vegetation physiological processes, such as ozone-induced damage, photosynthesis, and respiration (Lei et al., 2020). Additionally, it computes important land surface parameters, including CO₂ flux, BVOC emissions, and stomatal conductance (Yue and Unger, 2015). The YIBs model employs a leaf-level BVOC emission scheme based on vegetation photosynthesis. Unlike the traditional MEGAN (Model of Emissions of Gases and Aerosols from Nature) model, this approach incorporates the influence of plant photosynthesis on BVOC emissions, making it more representative of actual plant physiological processes. In this scheme, leaf-level BVOC emission rates depend on the photosynthetic rate, leaf surface temperature, and intracellular CO₂ concentration (Yue and Unger, 2015; Lei et al., 2020; Yue et al., 2015).

The RegCM-Chem and YIBs models exchange variables every 6 min, facilitating dynamic coupling between regional climate, atmospheric chemistry, and ecosystem processes. The RegCM-Chem-YIBs model simulated both primary and secondary PM_{2.5} emissions, including dust, black carbon, organic carbon, sulfates, nitrates, and ammonium. The structure of the model is shown in Fig. 1.

In the RegCM-Chem-YIBs model, changes in CO₂ concentrations affect PM_{2.5} primarily via two mechanisms: first, CO₂-induced radiative forcing alters the atmospheric radiation balance, leading to shifts in temperature, precipitation, and boundary-layer structure that modulate PM_{2.5} formation, transport, and removal (Li and Mölders, 2008; Matthews, 2007); and second, through the YIBs module, changes in CO₂ concentration modulate photosynthetic activity and stomatal behavior, altering BVOCs emissions that undergo atmospheric photochemical oxidation to form secondary organic aerosols, a significant fraction of PM_{2.5} (Kergoat et al., 2002; Kellomaki and Wang, 1998).

2.2 Model configurations

The study area covers the entire East Asian region, with a horizontal grid resolution of 60 km, centered at 36° N and 107° E. A terrain-following coordinate system was used vertically (Bleck and Benjamin, 1993), dividing the atmosphere into 18 layers from the surface to 50 hPa.

Anthropogenic pollutant emissions data were obtained from the Multi-resolution Emission Inventory for China (MEIC v1.4) developed by Tsinghua University (Geng et al., 2024). Surface CO2 flux data were sourced from the National Oceanic and Atmospheric Administration (NOAA) CarbonTracker CT2019 dataset, which includes contributions from fossil fuel combustion, biomass burning, and ocean-atmosphere CO₂ exchange (Peters et al., 2007). Meteorological fields were derived from ERA-Interim reanalysis (Balsamo et al., 2015), while sea surface temperature data were taken from NOAA's weekly mean dataset (Huang et al., 2021). The model employed the Grell cumulus parameterization scheme, the CCM3 radiation scheme, the Holtslag PBL scheme for boundary layers, the CBM-Z mechanism for meteorology and chemistry, and the TUV photochemistry scheme.

2.3 Experiment settings

The numerical experiments are presented in Table 1. The SIM₂₀₀₈ experiment represents the baseline conditions for the year 2008. In the SIM_{Base} experiment, interannual variations in meteorological fields, CO₂ emissions, and anthropogenic pollutant emissions (excluding CO₂ emissions) were considered for simulations spanning the period 2009–2018, representing the baseline conditions for those years. Additionally, the SIM_{MET=2008} and SIM_{CO₂=2008} experiments were designed, where meteorological fields and CO₂ emissions were fixed at their 2008 levels, while simulations were conducted for the 2009–2018 period. The simulation period spans from April to August each year. From this, the results from May to August, corresponding to the East Asian Summer Monsoon (EASM) period, were selected for analysis.

Changes in $PM_{2.5}$ concentrations were attributed to three main factors: anthropogenic pollutant emissions, meteorological conditions, and CO_2 variations. By comparing the simulation results from different years in the SIM_{Base} experiment to SIM_{2008} ($SIM_{Base} - SIM_{2008}$), we quantified changes in $PM_{2.5}$ concentrations relative to 2008 for the period 2009–2018. To evaluate the impact of meteorological conditions on $PM_{2.5}$ concentrations, we compared the results of the SIM_{Base} experiment with those of the $SIM_{MET=2008}$ experiment for the same year ($SIM_{Base} - SIM_{MET=2008}$). Similarly, the contribution of CO_2 emission changes to $PM_{2.5}$ variations was assessed by comparing the SIM_{Base} experiment with the $SIM_{CO_2=2008}$ experiment ($SIM_{Base} - SIM_{CO_2=2008}$) in the same year. The contribution of anthropogenic pollutant emissions was then determined by subtracting the effects

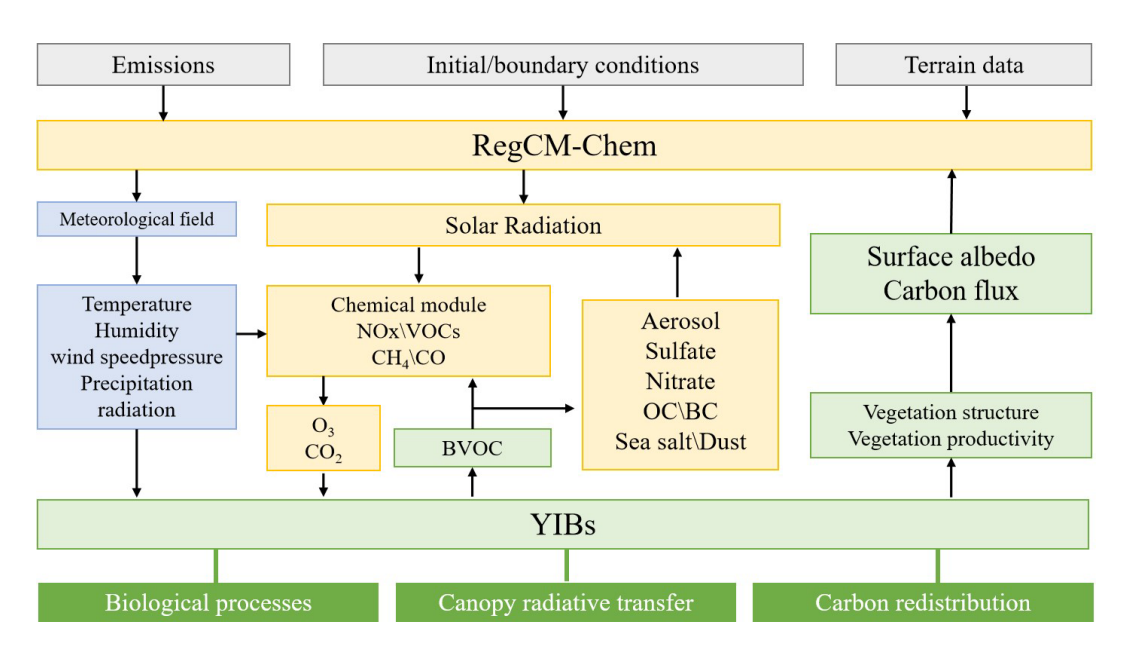


Figure 1. Framework of the RegCM-Chem-YIBs model.

of meteorological and CO_2 emission changes from the total $PM_{2.5}$ variation.

It is noteworthy that, as a principal greenhouse gas, CO_2 modifies meteorological parameters – such as radiation, temperature, and precipitation – which in turn influence $PM_{2.5}$ levels. In the comparison between experiments SIM_{Base} and $SIM_{CO_2=2008}$ ($SIM_{Base} - SIM_{CO_2=2008}$), all meteorological changes derive solely from variations in CO_2 emissions, a mechanism fundamentally different from the meteorological influences identified in experiments SIM_{Base} and $SIM_{MET=2008}$ ($SIM_{Base} - SIM_{MET=2008}$).

2.4 Model evaluations

Observed PM_{2.5} data were obtained from the China National Environmental Monitoring Center. This study used hourly PM_{2.5} concentrations during the summer monsoon period (1 May to 31 August) from 2015 to 2018. A total of 366 monitoring stations across Chinese cities, selected based on data completeness and representativeness, were used for model validation. The locations of these stations are shown in Fig. S5. CO₂ observations were sourced from the World Data Centre for Greenhouse Gases, including all seven sites in East Asia: Waliguan, Korea Tae-ahn Peninsula, Ulaanbaatar in Mongolia, Lulin, Yonagunijima, Cape D'Aguilar (Hong Kong), and King's Park. Detailed station locations are shown in Fig. S6. Reanalysis data for temperature, wind fields, and relative humidity were obtained from the ERA-Interim dataset.

As shown in Table 2 and Figs. S1-S6, the SIM_{Base} experiments reproduce 2015-2018 $PM_{2.5}$ and CO_2 concentrations with high correlations and low biases relative to observations, while their simulated meteorological fields closely match re-

analysis data. Overall, the RegCM-Chem-YIBs model effectively captures the fundamental characteristics and temporal trends of meteorological factors, PM_{2.5}, and CO₂ concentrations in East Asia (Ma et al., 2023a, b).

3 Results and discussion

3.1 PM_{2.5} variation

Changes in PM_{2.5} concentrations from 2009 to 2018 relative to 2008 were quantified by comparing simulation results from each year in the SIM_{Base} experiment with SIM₂₀₀₈ (SIM_{Base} – SIM₂₀₀₈). Figure 2 illustrates the changes in nearsurface PM_{2.5} concentrations across East Asia from 2009 to 2018. PM_{2.5} concentrations are notably higher in the North China Plain, northeastern China, and eastern China (Shanghai, Jiangsu, Zhejiang), largely driven by industrial emissions, vehicle exhaust, coal combustion, and dust from human activities (Wang et al., 2017). In contrast, regions in western China (Yunnan, Gansu, Xinjiang) exhibit lower PM_{2.5} levels due to limited industrial activity, lower population density, and more favorable meteorological conditions (low water vapor content, lower temperatures, and weak solar radiation are unfavorable for the formation of secondary aerosols such as sulfates, nitrates, and organic aerosols) (Wei et al., 2021; Xue et al., 2020). Developed cities and industrial centers like the PRD and Fuzhou (Fujian Province) continue to encounter challenges related to PM_{2.5} pollution. Moreover, the Sichuan region, characterized by its enclosed basin geography and high population density, also experiences high PM_{2.5} pollution levels (Wang et al., 2018b). From 2009 to 2013, PM_{2.5} concentrations in China remained relatively stable, with levels averaging around 90 µg m⁻³ in the

Table 1. The numerical experimental in this study.

Experiment	Time	Meteorological fields	CO ₂ emissions	Anthropogenic pollutant emissions
SIM ₂₀₀₈	2008	2008	2008	2008
SIM _{Base}	2009–2018	2009–2018	2009–2018	2009–2018
SIM _{MET=2008}	2009–2018	2008	2009–2018	2009–2018
SIM _{CO2=2008}	2009–2018	2009–2018	2008	2009–2018

Table 2. Evaluations of the near-surface CO₂ and PM_{2.5} in East Asia.

Species	Year	Observation	Simulation	Bias	RMSE	R
CO ₂ (ppm)	2015	402.82	406.98	4.16	9.37	0.44
	2016	407.12	410.44	3.32	8.22	0.69
	2017	408.35	413.62	5.27	11	0.39
	2018	409.61	416.68	7.07	11.32	0.41
$PM_{2.5} (\mu g m^{-3})$	2015	36.6	25.57	-11.03	12.99	0.71
	2016	31.03	22.91	-8.12	10.31	0.64
	2017	29.61	24.02	-5.59	10.57	0.71
	2018	27.18	19.04	-8.14	11.62	0.61

RMSE: root mean square error; R: correlation coefficient.

North China Plain and the Sichuan Basin (SCB). However, following the implementation of the Clean Air Action Plan in 2013, $PM_{2.5}$ levels significantly declined nationwide. By 2018, concentrations had dropped to below $50 \, \mu g \, m^{-3}$ across much of the country.

Figure 3 and Table 3 present the changes in PM_{2.5} concentrations relative to 2008 across East Asia from 2009 to 2018. Since 2008, most regions in China have seen varying degrees of PM_{2.5} reduction. During the pre-governance (PreG) period (2009–2013), the largest decrease occurred in the YRD, with a reduction of $14.77 \,\mu\mathrm{g}\,\mathrm{m}^{-3}$, followed by the SCB and PRD, where concentrations dropped by 10.59 and $8.69 \,\mu g \,m^{-3}$, respectively. In contrast, the Fenwei Plain (FWP) and PRD experienced smaller changes, with reductions of less than $3 \,\mu \mathrm{g} \,\mathrm{m}^{-3}$. PM_{2.5} concentrations across China significantly decreased after the implementation of the Clean Air Action Plan in 2013. The most notable reductions were simulated in the North China Plain and SCB, where PM2.5 concentrations dropped by 36.76 and 33.96 $\mu g m^{-3}$, respectively. In the FWP and YRD, PM_{2.5} concentrations decreased by 22.16 to $27.89 \,\mu g \, m^{-3}$. In contrast, the PRD saw a smaller reduction, with levels decreasing by just $8.03 \,\mu \mathrm{g} \,\mathrm{m}^{-3}$. This may be attributed to the region's significant influence from the summer monsoon and relatively lower impact from anthropogenic pollutant emissions. Further analysis of these factors will be conducted in subsequent sections.

Table S1 shows that the mean $PM_{2.5}$ trend over China during the PreG (2009–2013) and post-governance (PostG; 2014–2018) periods was -1.84 and $-2.90 \,\mu g \, m^{-3} \, yr^{-1}$, respectively. These values are consistent with the findings of Silver et al. (2025), who reported a $PM_{2.5}$ trend

of $-2.47\,\mu g\,m^{-3}\,yr^{-1}$ for 2014–2017 in China based on ground-based observations. Similarly, Lin et al. (2018) reported PM_{2.5} trends of -0.65 and $-2.30\,\mu g\,m^{-3}\,yr^{-1}$ for 2006–2010 and 2011–2015 in China, respectively. Using satellite remote sensing data, Ma et al. (2019) found declines of 1.03 and 4.27 $\mu g\,m^{-3}\,yr^{-1}$ for 2010–2013 and 2013–2017 in China, respectively. The high-resolution Chinese air quality reanalysis developed by Kong et al. (2021) using data assimilation techniques indicated a more pronounced decline of $-5.80\,\mu g\,m^{-3}\,yr^{-1}$ for PM_{2.5} from 2013 to 2018 in China. In addition, Silver et al. (2018), based on multi-source data, reported a trend of $-3.40\,\mu g\,m^{-3}\,yr^{-1}$ for 2015–2017 in China. Therefore, our simulation accurately captures the observed PM_{2.5} trends over China from 2008 to 2018, providing a robust foundation for subsequent attribution analyses.

Overall, before 2013, near-surface $PM_{2.5}$ concentrations across China showed little variation. However, after 2013, a significant reduction in $PM_{2.5}$ pollution levels was simulated nationwide. Changes in $PM_{2.5}$ concentrations were attributed to three main factors: anthropogenic pollutant emissions, meteorological conditions, and CO_2 variations. The following sections analyze each factor's contribution to the changes in $PM_{2.5}$ concentrations from 2008 to 2018.

3.2 Contribution of meteorological conditions

The impact of meteorological conditions variations on $PM_{2.5}$ concentrations were assessed by comparing SIM_{Base} results with those from $SIM_{MET=2008}$ for the same year ($SIM_{Base} - SIM_{MET=2008}$). As shown in Fig. 4, during the PreG period, precipitation increased by 2–4 mm d⁻¹ in China's east-

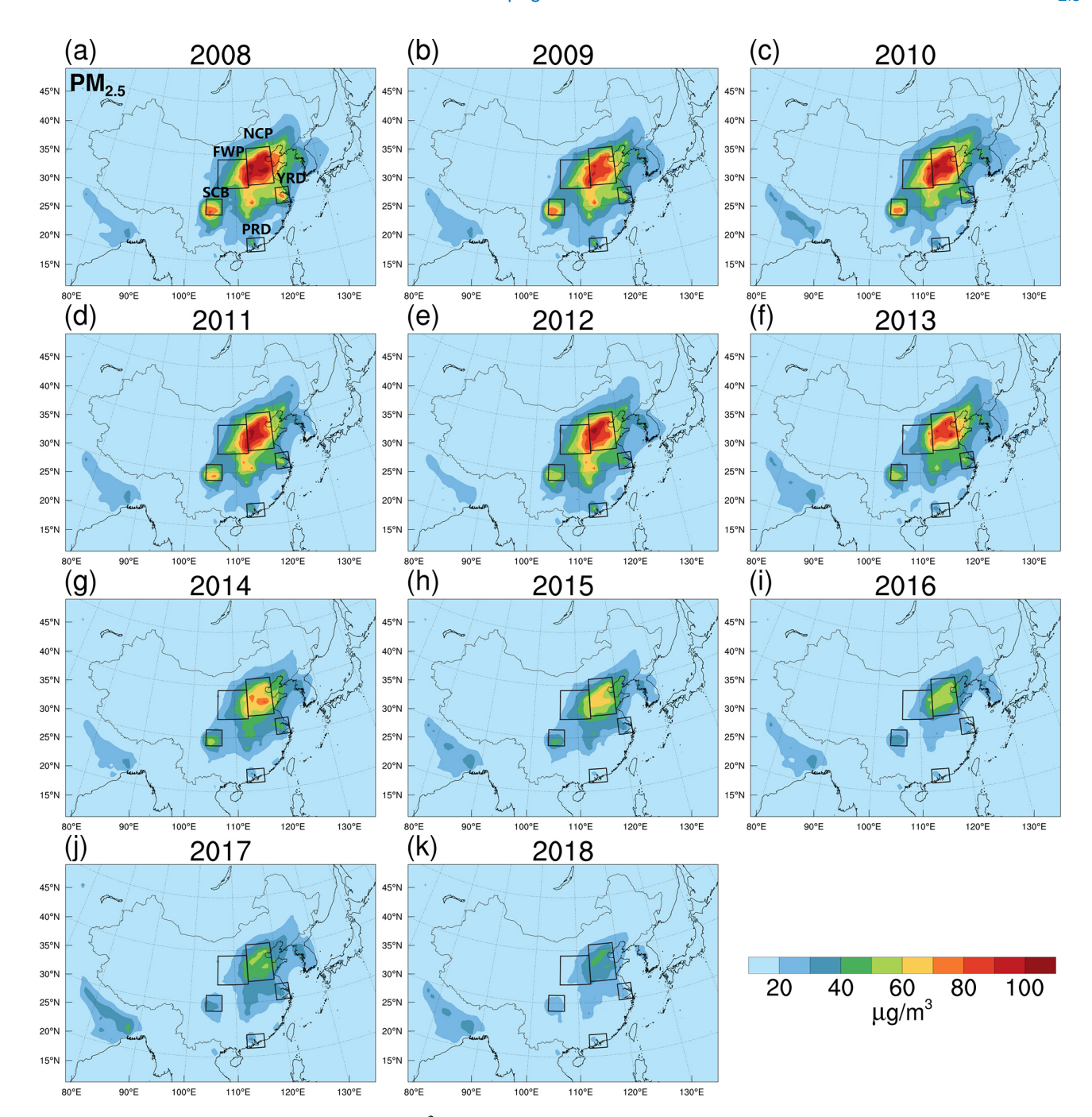


Figure 2. Near-surface $PM_{2.5}$ concentrations ($\mu g \, m^{-3}$) over East Asia during the EASM period from 2009 (a) to 2018 (k) (SIM_{2008}). Key regions are highlighted by black boxes, including the North China Plain (NCP), Fenwei Plain (FWP), Yangtze River Delta (YRD), Pearl River Delta (PRD), and Sichuan Basin (SCB).

ern coastal and western inland regions, while it decreased by approximately $2 \, \text{mm} \, \text{d}^{-1}$ in central China. This increase in precipitation facilitates the reduction of near-surface $PM_{2.5}$ concentrations through wet deposition. Consequently, trends in $PM_{2.5}$ concentrations are inversely related to precipitation: concentrations decreased by $2{\text -}16\,\mu\text{g}\,\text{m}^{-3}$ in the eastern coastal and western inland regions, while they increased by

4–8 μg m⁻³ around 110° E in central China. Additionally, in northeastern and southwestern China, wind speeds increased by 1 to 2 m s⁻¹, contributing to the reduction of PM_{2.5} concentrations. In contrast, decreased wind speeds in southeastern and central China facilitated the accumulation of PM_{2.5}. During the PostG period, the significant increase in temperature (Fig. 4l) promoted the formation of PM_{2.5}, leading to

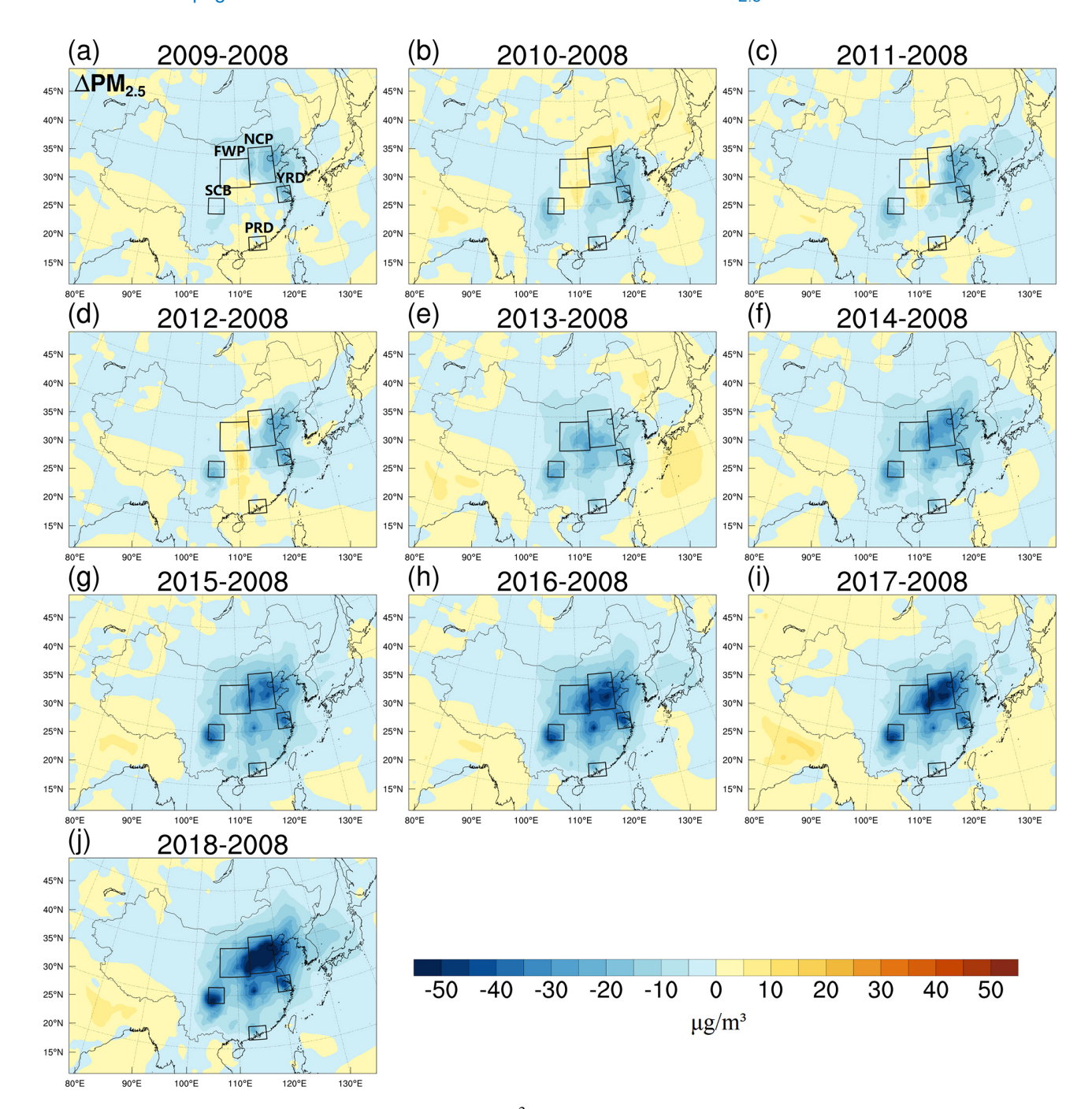


Figure 3. Changes in near-surface $PM_{2.5}$ concentrations ($\mu g \, m^{-3}$) during the EASM period from 2009 (a) to 2018 (j) relative to 2008 in East Asia ($SIM_{Base} - SIM_{2008}$).

an expansion of the areas where $PM_{2.5}$ concentrations increased. Overall, $PM_{2.5}$ concentrations have decreased in the eastern coastal and western inland regions but increased in the central area of China.

Table 4 indicates that in the North China Plain (NCP) region precipitation increased by 0.58 to $0.6\,\mathrm{mm\,d^{-1}}$ and wind speed rose by 0.17 to $0.26\,\mathrm{m\,s^{-1}}$ during the PreG and PostG periods, resulting in a decrease in near-surface PM_{2.5}

concentrations of 1.6 to $4.01\,\mu g\,m^{-3}$. In the FWP region, PM_{2.5} concentrations increased by 1 to $2.31\,\mu g\,m^{-3}$, which was associated with a rise in temperature of 0.1 to 0.46 K and a significant decrease in PBLH of 108.5 to 15.3 m. In the YRD region, the increase in wind speed of 0.48 to $1.02\,m\,s^{-1}$ facilitated a reduction in PM_{2.5} concentrations by 0.43 to 0.61 $\mu g\,m^{-3}$. Conversely, in the PRD region, reduced precipitation combined with increased temperature

Table 3. Changes in near-surface $PM_{2.5}$ concentrations ($\mu g m^{-3}$) during the EASM period from 2009 to 2018 relative to 2008 in the North China Plain (NCP), Fenwei Plain (FWP), Yangtze River Delta (YRD), Pearl River Delta (PRD), and Sichuan Basin (SCB) (SIM_{Base} – SIM₂₀₀₈).

Year	NCP	FWP	YRD	PRD	SCB
2009	-11.24	-1.29	-11.37	1.41	-3.16
2010	-3.87	1.9	-15.2	-3.57	-4.79
2011	-6.27	0.22	-14.76	0.13	-8.65
2012	-7.42	1.69	-17.61	2.35	-15.99
2013	-14.67	-15.49	-14.9	-6.34	-20.37
2014	-24.26	-15.36	-19.95	-6.72	-22.87
2015	-31.41	-16.9	-27.76	-9.91	-31.75
2016	-38.5	-25.23	-32.43	-8.18	-35.58
2017	-40.69	-25.49	-26.21	-5.82	-37.43
2018	-48.96	-27.83	-33.08	-9.53	-42.19
PreG	-8.69	-2.59	-14.77	-1.20	-10.59
PostG	-36.76	-22.16	-27.89	-8.03	-33.96

contributed to an increase in $PM_{2.5}$ concentrations, ranging from 0.11 to $1.49 \,\mu g \, m^{-3}$. In the SCB region, $PM_{2.5}$ concentrations rose by $0.29 \,\mu g \, m^{-3}$ during the PreG period, which can be linked to a significant decrease in PBLH of 136.5 m. In the PostG period, $PM_{2.5}$ concentrations decreased by $1.14 \,\mu g \, m^{-3}$, which can be attributed to an increase in precipitation $(0.37 \, mm \, d^{-1})$ and a decrease in temperature $(0.14 \, K)$.

3.3 Contribution of CO₂

The contribution of CO_2 emission changes to $PM_{2.5}$ variability was quantified by comparing the SIM_{Base} experiment with the $SIM_{CO_2=2008}$ experiment ($SIM_{Base} - SIM_{CO_2=2008}$) within the same year. As shown in Fig. 5, following the ongoing urbanization and industrialization, CO_2 concentrations across East Asia rose by 2–10 ppm during both the PreG and PostG periods, with a sharper increase in the PostG period. CO_2 influences atmospheric $PM_{2.5}$ concentrations both through its radiative effects on precipitation and by altering BVOC emissions from vegetation. Overall, CO_2 changes contributed to $PM_{2.5}$ variations across East Asia from 2008 to 2018, ranging from -4 to $6\,\mu g\,m^{-3}$. $PM_{2.5}$ pollution levels generally increased in the PreG period, while reductions were more common in the PostG period.

Table 5 presents a detailed analysis of the five target regions. In northern China, particularly the NCP and FWP regions, limited vegetation coverage means CO_2 impacts surface $PM_{2.5}$ concentrations mainly through precipitation changes. In the PostG period, precipitation increased by $0.06-0.13~\mathrm{mm}~\mathrm{d}^{-1}$, lowering $PM_{2.5}$ concentrations by $0.98-1.3~\mu\mathrm{g}~\mathrm{m}^{-3}$. Similarly, in the SCB, precipitation rose by $0.21-0.64~\mathrm{mm}~\mathrm{d}^{-1}$, reducing $PM_{2.5}$ concentrations by $0.49-0.73~\mu\mathrm{g}~\mathrm{m}^{-3}$ in the PreG and PostG periods. However, in the YRD and PRD regions, where vegetation coverage is higher,

CO₂ primarily impacts PM_{2.5} concentrations by modulating BVOC emissions. The impact can be either positive or negative (Possell et al., 2005) depending primarily on the balance between the inhibitory effects on synthase activity and the stimulatory effects of enhanced photosynthesis (Wilkinson et al., 2009). In the YRD region, isoprene fell by 0.32–0.58 $\mu g\,m^{-3}$ during both periods, while precipitation rose by 0.09–0.13 mm d $^{-1}$, collectively reducing PM_{2.5} by 0.02–0.05 $\mu g\,m^{-3}$. In the PRD region, isoprene concentrations increased significantly by 0.31–0.92 $\mu g\,m^{-3}$, while precipitation decreased by 0.33–1.02 mm d $^{-1}$. Consequently, PM_{2.5} concentrations rose by 0.31–1.13 $\mu g\,m^{-3}$ during both the PreG and PostG periods.

3.4 Contribution of anthropogenic pollutant emissions

The contribution of changed anthropogenic pollutant emissions to PM_{2.5} variation was determined by removing the effects of meteorological and CO₂ emission changes from the total variation. Figure 6 illustrates a significant downward trend in PM_{2.5} concentrations across East Asia since 2008. During the PreG period, PM_{2.5} levels decreased by an average of 5 to $10 \,\mu \mathrm{g} \,\mathrm{m}^{-3}$ over East Asia. Following the implementation of the Clean Air Action Plan in 2013, a marked reduction in PM_{2.5} concentrations was simulated. The most substantial decreases, of approximately 60 µg m⁻³, occurred in the NCP and SCB regions. Anthropogenic pollutant emissions emerged as the primary drivers of this decline, with their spatial distribution and magnitude of impact closely corresponding to the overall changes in PM2.5 concentrations. In contrast, the effects of changing meteorological conditions and CO₂ emissions on PM_{2.5} levels in East Asia were relatively minor, ranging between -5 and $5 \,\mu \mathrm{g} \,\mathrm{m}^{-3}$. Meteorological conditions have reduced PM2.5 concentrations in the eastern coastal and western regions of China, while increasing them in the central region. In the PostG period, the extent of PM_{2.5} concentration increases has expanded. The impact of CO₂ emission changes on PM_{2.5} levels shows different trends in the PreG and PostG periods. In the PreG period, changes in CO₂ emissions primarily led to an increase in PM_{2.5} concentrations. However, in the PostG period, the rise in CO₂ concentrations began to have a negative impact, leading to a reduction in PM_{2.5} concentrations.

Based on Fig. 7 and Table 6, $PM_{2.5}$ concentrations in the NCP region decreased by $5.28 \, \mu g \, m^{-3}$ during the PreG period and by $33.86 \, \mu g \, m^{-3}$ in the PostG period. Anthropogenic pollutant emissions were the primary driver of these changes. During the PreG period, the influence of meteorological conditions on $PM_{2.5}$ was comparable to that of anthropogenic pollutant emissions, with changes in meteorology contributing $-4.01 \, \mu g \, m^{-3}$ and emissions contributing $-5.28 \, \mu g \, m^{-3}$. However, in the PostG period, the impact of meteorological factors diminished to $-1.6 \, \mu g \, m^{-3}$, indicating that anthropogenic pollutant emissions became the predominant factor in the reduction of $PM_{2.5}$ concentrations. In contrast, the ef-

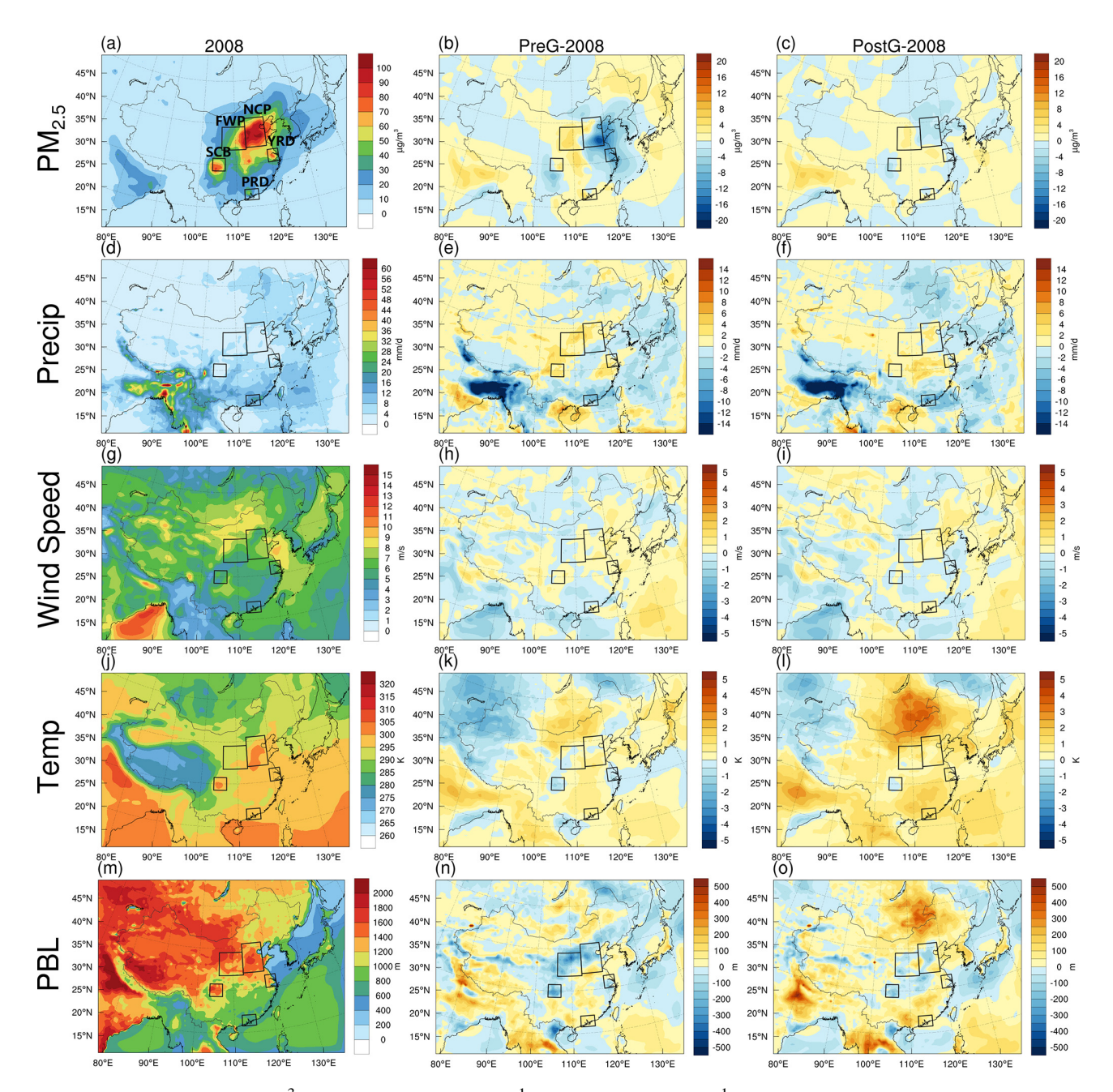


Figure 4. The PM_{2.5} (a–c, μ g m⁻³), precipitation (d–f, mm d⁻¹), wind speed (g–i, m s⁻¹), temperature (j–l, K), and planetary boundary layer (PBL) height (m–o, m) during the EASM period in 2008 (left), and their mean changes due to meteorological variations in the PreG (2009–2013, center) and PostG (2014–2018, right) periods relative to 2008. PreG-2008 and PostG-2008 represent the average annual differences between experiments SIM_{Base} and SIM_{MET=2008} (SIM_{Base} – SIM_{MET=2008}) for the periods 2009–2013 and 2014–2018, respectively.

fect of changes in CO_2 emissions on $PM_{2.5}$ levels was relatively minor, ranging from -1.3 to $0.6 \,\mu g \, m^{-3}$.

The situation in the FWP region is similar to that of the NCP region, with anthropogenic pollutant emissions as the primary driver of reduced $PM_{2.5}$ concentrations. During the PreG and PostG periods, the contributions of anthropogenic pollutant emissions to $PM_{2.5}$ levels were -5.75 and $-22.18 \, \mu g \, m^{-3}$, respectively. In contrast, meteorologi-

cal conditions contributed to an increase in $PM_{2.5}$ concentrations, with a contribution of $2.32\,\mu g\,m^{-3}$ in the PreG period, comparable to the impact of anthropogenic pollutant emissions. Meanwhile, the influence of CO_2 emissions on $PM_{2.5}$ levels was relatively minor.

In the YRD region, anthropogenic pollutant emissions are the primary driver of reduced PM_{2.5} concentrations. Due to its location in eastern China, the YRD region is more af-

Table 4. Impact of meteorological condition changes on $PM_{2.5}$ ($\mu g \, m^{-3}$), precipitation (mm d⁻¹), wind speed (m s⁻¹), near-surface temperature (K), and planetary boundary layer (PBL) height (m) during the EASM period in the PreG (2009–2013) and PostG (2014–2018) periods relative to 2008. PreG and PostG represent the average annual differences between experiments SIM_{Base} and $SIM_{MET=2008}$ ($SIM_{Base} - SIM_{MET=2008}$) for the periods 2009–2013 and 2014–2018, respectively.

Region	Period	$PM_{2.5} \ (\mu g m^{-3})$	Precipitation $(mm d^{-1})$	Wind speed (m s ⁻¹)	Near-surface temperature (K)	PBL (m)
NCP	PreG PostG	-4.01 -1.6	0.58 0.6	0.17 0.26	0.32 0.6	-46.8 -14.5
FWP	PreG PostG	2.32	1.68 0.81	-0.06 0.05	0.1 0.46	-108.5 -15.3
YRD	PreG PostG	-6.31 -0.43	1.02 0.48	0.18 -0.08	-0.29 0.45	-33.9 21.9
PRD	PreG PostG	1.49 0.11	-2.39 -3.24	-0.02 0.18	0.36 1.00	29.6 52.2
SCB	PreG PostG	0.29 -1.14	1.81 0.37	0.13 -0.03	-0.58 -0.14	-136.5 -76

Table 5. Impact of CO_2 emission changes on $PM_{2.5}$ (μ g m⁻³), CO_2 (ppm), precipitation (mm d⁻¹), and isoprene (μ g m⁻³) during the EASM period in the PreG (2009–2013) and PostG (2014–2018) periods relative to 2008. PreG and PostG represent the average annual differences between experiments SIM_{Base} and $SIM_{CO_2=2008}$ ($SIM_{Base} - SIM_{CO_2=2008}$) for the periods 2009–2013 and 2014–2018, respectively.

Region	Period	$PM_{2.5}$ (µg m ⁻³)	CO ₂ (ppm)	Precipitation $(mm d^{-1})$	Isoprene (μg m ⁻³)
NCP	PreG	0.6	3.19	0.27	-0.1
	PostG	-1.3	4.24	0.13	0.26
FWP	PreG	0.84	1.70	0.21	-0.16
	PostG	-0.98	2.05	0.06	0.33
YRD	PreG	-0.02	4.1	0.13	-0.32
	PostG	-0.05	6.2	0.09	-0.58
PRD	PreG	1.13	1.97	-1.02	0.31
	PostG	0.31	3.20	-0.33	0.92
SCB	PreG	-0.49	2.80	0.64	-0.78
	PostG	-0.73	2.78	0.21	0.69

fected by the EASM, resulting in more pronounced effects of changing meteorological conditions on PM_{2.5} levels compared to the NCP and FWP regions. During the PreG period, the impact of meteorological conditions on PM_{2.5} concentrations reached as high as $-6.31\,\mu\mathrm{g\,m^{-3}}$.

In the PRD region, changes in anthropogenic pollutant emissions have contributed to a reduction in $PM_{2.5}$ concentrations, ranging from -8.45 to $-3.82 \,\mu g \, m^{-3}$. However, changes in meteorological conditions and CO_2 emissions have led to increases in $PM_{2.5}$ levels, ranging from 0.11 to $1.49 \,\mu g \, m^{-3}$. Similar to the YRD region, the effects of changing meteorological conditions on $PM_{2.5}$ concentrations are significant, peaking at $1.49 \,\mu g \, m^{-3}$ during the PreG period. Located in southeastern coastal China, the PRD's rich vege-

tation cover enhances the impact of CO_2 emission changes on $PM_{2.5}$ concentrations. During the PreG period, the influence of CO_2 emission changes on $PM_{2.5}$ levels reached $1.13 \, \mu g \, m^{-3}$, comparable to the effect of anthropogenic pollutant emissions ($-3.82 \, \mu g \, m^{-3}$). In the PostG period, the impact of CO_2 emission changes ($0.31 \, \mu g \, m^{-3}$) surpassed that of meteorological conditions ($0.11 \, \mu g \, m^{-3}$).

In the SCB region, the basin topography results in relatively minor effects of meteorological conditions and CO_2 emission changes on $PM_{2.5}$ levels, with contributions ranging from -1.14 to $0.29 \, \mu \mathrm{g \, m^{-3}}$ during both the PreG and PostG periods. In contrast, anthropogenic pollutant emissions are the primary drivers of reduced $PM_{2.5}$ concentra-

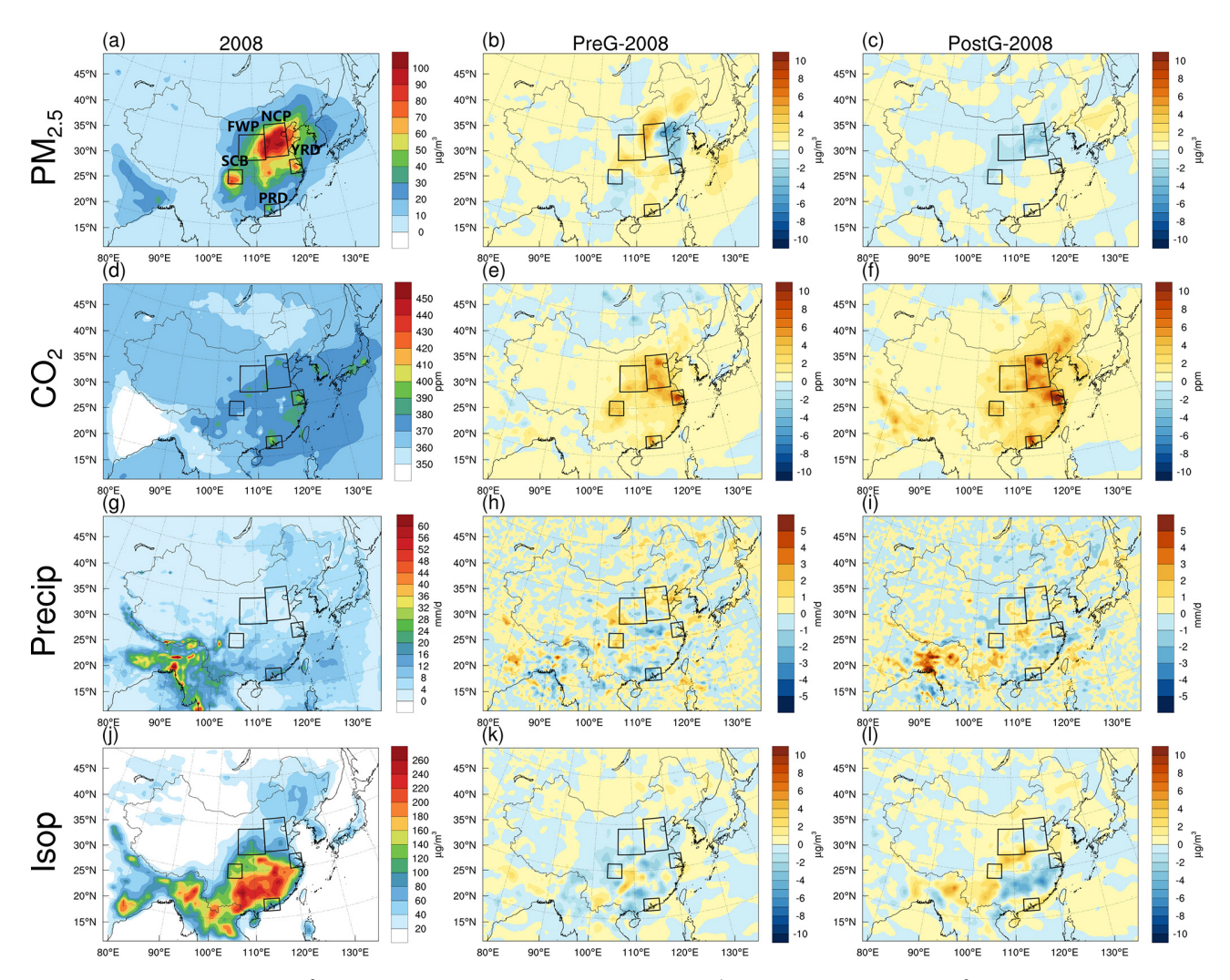


Figure 5. The $PM_{2.5}$ (a-c, μ g m⁻³), CO_2 (d-f, ppm), precipitation (g-i, mm d⁻¹), and isoprene (j-l, μ g m⁻³) during the EASM period in 2008 (left) and their mean changes due to CO_2 emission variations in the PreG (2009–2013, center) and PostG (2014–2018, right) periods relative to 2008. PreG-2008 and PostG-2008 represent the average annual differences between experiments SIM_{Base} and $SIM_{CO_2=2008}$ ($SIM_{Base} - SIM_{CO_2=2008}$) for the periods 2009–2013 and 2014–2018, respectively.

tions, exerting an impact of $-32.09 \,\mu\mathrm{g}\,\mathrm{m}^{-3}$ during the PostG period.

3.5 Attribution of changes in PM_{2.5}

Figure 8 illustrates that PM_{2.5} concentrations remained relatively stable across the five regions during the PreG period. However, in the PostG period, following the implementation of the Clean Air Action Plan, significant reductions in PM_{2.5} concentrations were simulated in the NCP, FWP, YRD, and SCB regions, while the PRD region showed the smallest decrease.

Anthropogenic pollutant emissions are the primary factor driving PM_{2.5} concentration reductions across the five regions, with their impact increasing linearly over time. In the PreG period, meteorological conditions had a rela-

tively stronger influence on PM_{2.5} levels, occasionally surpassing the effects of anthropogenic pollutant emissions. For example, in 2013, the meteorological and emission impacts on PM_{2.5} in the NCP region were -17.35 and $4.49\,\mu g\,m^{-3}$, respectively. Similarly, in the FWP region from 2013 to 2015, meteorological impacts ranged from -16.9 to $-15.36\,\mu g\,m^{-3}$, while emissions affected PM_{2.5} concentrations between -15.8 and $-2.27\,\mu g\,m^{-3}$. The influence of meteorology also exceeded that of emissions in the YRD region during 2011–2012 and in the PRD region in 2010. Even in the SCB region, where meteorological impacts on PM_{2.5} were relatively minor, meteorological effects in 2010 (8.59 $\mu g\,m^{-3}$) were comparable to emissions $(-14.67\,\mu g\,m^{-3})$.

The influence of CO₂ emission changes on PM_{2.5} levels was generally minor, but in the densely vegetated PRD re-

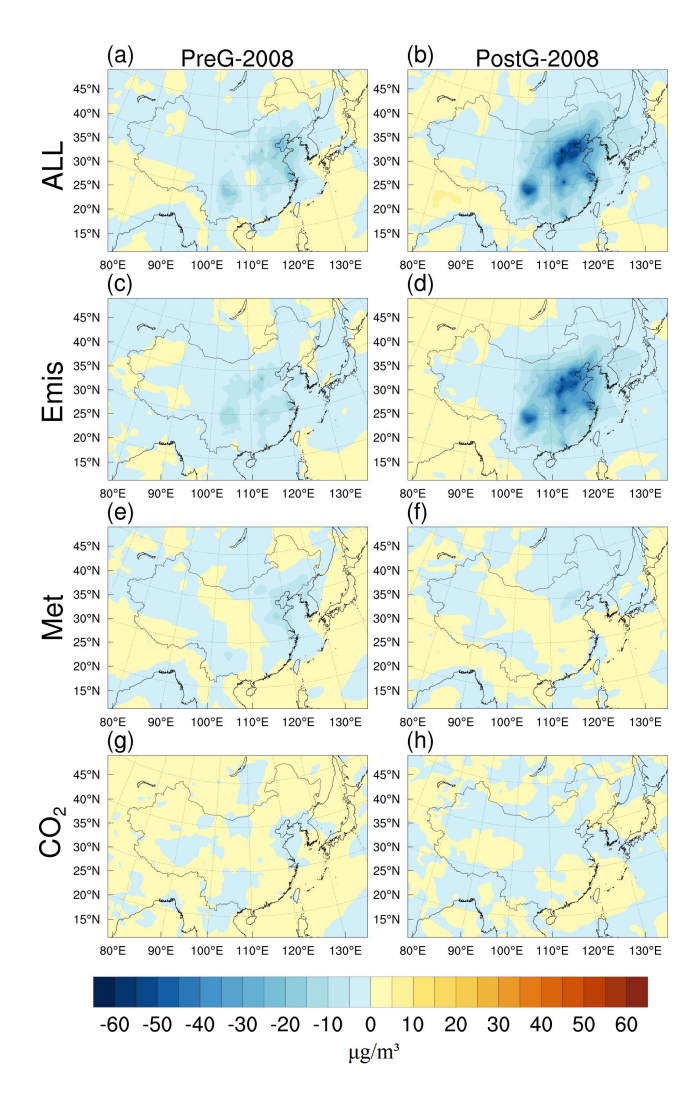


Figure 6. The total changes in $PM_{2.5}$ concentrations (All, $SIM_{Base} - SIM_{2008}$), and the changes in $PM_{2.5}$ attributed to variations of anthropogenic pollutant emissions (Emis, All-Met-CO₂), meteorological conditions (Met, $SIM_{Base} - SIM_{MET=2008}$), and CO_2 emissions (CO₂, $SIM_{Base} - SIM_{CO_2=2008}$) during the EASM period in the PreG (2009–2013, left) and PostG (2014–2018, right) periods relative to 2008.

gion could be comparable to the effects of emissions and meteorology. The influences of CO_2 emissions, anthropogenic pollutant emissions, and meteorology on $PM_{2.5}$ are -0.25 to 3.11, -6.19 to -1.47, and -0.5 to $3.11 \,\mu g \, m^{-3}$, respectively from 2009 to 2013.

Our attribution analysis of $PM_{2.5}$ concentration changes is mainly consistent with previous studies, which have indicated that variations in anthropogenic pollutant emissions were the primary driver of $PM_{2.5}$ changes in China during the period 2013–2017, with meteorological conditions contributing approximately 9 %–26 % (Zhang et al., 2019; Chen et al., 2020a; Cheng et al., 2019). In our study, relative to 2008, the average contribution of anthropogenic pollutant

Table 6. Changes in total $PM_{2.5}$ concentrations (ALL, $SIM_{Base} - SIM_{2008}$) and the impacts of anthropogenic pollutant emissions (Emis, All-Met-CO₂), meteorological conditions (Met, $SIM_{Base} - SIM_{MET=2008}$), and CO_2 emission (CO_2 , $SIM_{Base} - SIM_{CO_2=2008}$) variations on $PM_{2.5}$ concentrations (µg m⁻³) during the EASM period in the PreG (2009–2013) and PostG (2014–2018) periods relative to 2008.

Period	ALL	Emis	Met	CO ₂
PreG	-8.69	-5.28	-4.01	0.6
PostG	-36.76	-33.86	-1.6	-1.3
PreG	-2.59	-5.75	2.32	0.84
PostG	-22.16	-22.18	1	-0.98
PreG	-14.77	-8.44	-6.31	-0.02
PostG	-27.89	-27.41	-0.43	-0.05
PreG	-1.2	-3.82	1.49	1.13
PostG	-8.03	-8.45	0.11	0.31
PreG	-10.59	-10.39	0.29	-0.49
PostG	-33.96	-32.09	-1.14	-0.73
	PreG PostG PreG PostG PreG PostG PreG PostG	PreG -8.69 PostG -36.76 PreG -2.59 PostG -22.16 PreG -14.77 PostG -27.89 PreG -1.2 PostG -8.03 PreG -10.59	PreG -8.69 -5.28 PostG -36.76 -33.86 PreG -2.59 -5.75 PostG -22.16 -22.18 PreG -14.77 -8.44 PostG -27.89 -27.41 PreG -1.2 -3.82 PostG -8.03 -8.45 PreG -10.59 -10.39	PreG -8.69 -5.28 -4.01 PostG -36.76 -33.86 -1.6 PreG -2.59 -5.75 2.32 PostG -22.16 -22.18 1 PreG -14.77 -8.44 -6.31 PostG -27.89 -27.41 -0.43 PreG -1.2 -3.82 1.49 PostG -8.03 -8.45 0.11 PreG -10.59 -10.39 0.29

emissions during the PreG period was 89.08%, while meteorological conditions contributed 16.45%. In the PostG period, following the implementation of the Clean Air Action Plan, the influence of anthropogenic pollutant emissions further increased to 96.26%, whereas the contribution of meteorological conditions declined to 1.60%. This finding underscores that the impact of changes in anthropogenic pollutant emissions on PM_{2.5} concentrations was markedly enhanced after 2013. Notably, changes in CO₂ emissions had a significant impact on PM_{2.5} levels, contributing -5.46% during the PreG period and 2.14% during the PostG period, with the latter effect surpassing that of meteorological conditions.

3.6 Uncertainties

The uncertainties in the MEIC emission inventory primarily arise from activity data, emission factors, spatial and temporal allocation methods, and the implementation status of pollution control measures (Hong et al., 2017; Zheng et al., 2021a), all of which may affect the accuracy of simulation results. Future improvements can be achieved by employing more refined and accurate emission inventories.

In addition, the use of a 60 km low-resolution grid limits the ability to represent local topography and physical processes, thereby introducing simulation errors (Harris et al., 2016; Ringler et al., 2013). Given that this study employs a fully coupled regional climate–chemistry–ecology model with extended simulation periods (three sets of 10-year simulations) and a broad regional scope (covering the entire East Asia region), computational resource constraints necessitated the use of 60 km grids. Numerous studies have employed the RegCM-Chem-YIBs model at a 60 km grid resolution to sys-

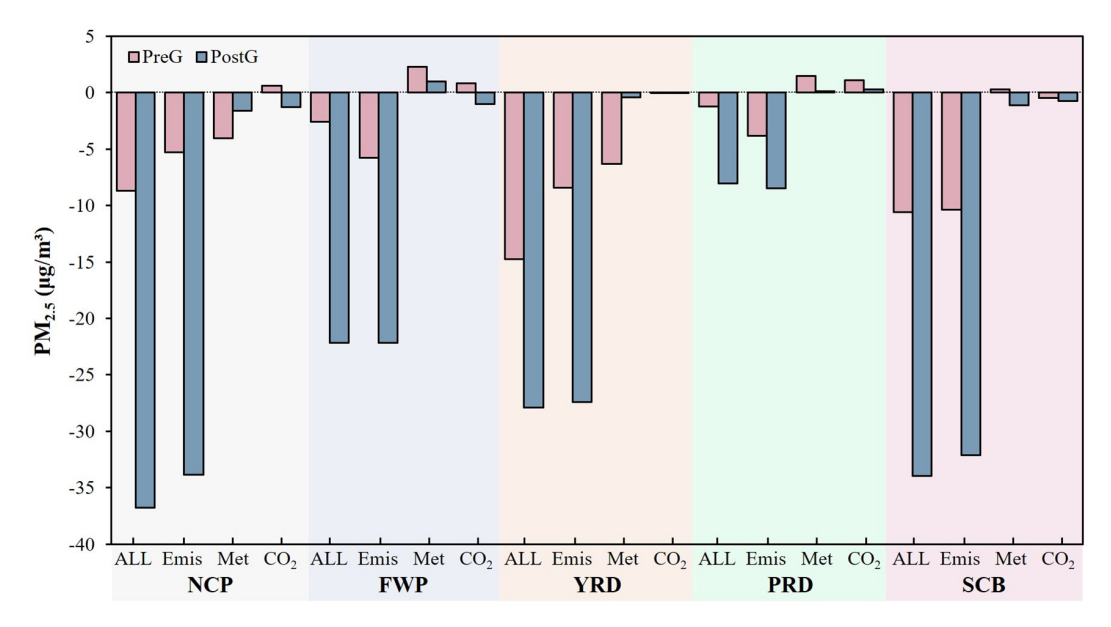


Figure 7. The total changes in $PM_{2.5}$ concentrations (All, $SIM_{Base} - SIM_{2008}$) for the North China Plain (NCP), Fenwei Plain (FWP), Yangtze River Delta (YRD), Pearl River Delta (PRD), and Sichuan Basin (SCB) during the EASM period in the PreG (2009–2013) and PostG (2014–2018) periods relative to 2008, along with the variations in $PM_{2.5}$ due to anthropogenic pollutant emissions (Emis, All-Met-CO₂), meteorological conditions (Met, $SIM_{Base} - SIM_{MET=2008}$), and CO_2 emission (CO₂, $SIM_{Base} - SIM_{CO_2=2008}$) changes.

tematically analyze PM_{2.5}, O₃, CO₂, and the regional climate over East Asia (Ma et al., 2023a, b; Xu et al., 2023; Gao et al., 2021). These demonstrate its robustness and reliability in simulating East Asian atmospheric and climatic conditions. Future studies could enhance simulation accuracy by increasing computational resources and employing higher-resolution grids.

4 Conclusions

This study employed numerical experiments with the RegCM-Chem-YIBs model to analyze the interannual variability of near-surface PM_{2.5} concentrations in East Asia from 2008 to 2018. The analysis examines the drivers of annual PM_{2.5} changes in detail, focusing on three key factors: anthropogenic pollutant emissions, meteorological conditions, and CO₂ concentration changes.

Compared to 2008, $PM_{2.5}$ concentrations in East Asia exhibited minimal change during the PreG period, with most areas showing variations between -10 and $5 \,\mu g \, m^{-3}$. In contrast, following the implementation of the Clean Air Action Plan, $PM_{2.5}$ concentrations decreased significantly (the PostG period). This reduction was especially notable in the NCP and the SCB regions, with declines of 36.76 and $33.96 \,\mu g \, m^{-3}$, respectively.

Anthropogenic pollutant emissions are the primary driver of the decline in $PM_{2.5}$ concentrations in East Asia, with their impact on $PM_{2.5}$ levels increasing linearly over time. During the PreG and PostG periods, the contributions of anthropogenic pollutant emissions to $PM_{2.5}$ concentrations in

the NCP, FWP, YRD, PRD, and SCB regions ranged from -10.39 to -3.82 and -33.86 to $-8.45 \,\mu g \, m^{-3}$, respectively.

Changes in meteorological conditions have led to decreased $PM_{2.5}$ concentrations along China's eastern coastal and western inland regions, while increasing $PM_{2.5}$ levels in central areas. During the PreG period, the influence of these meteorological changes on $PM_{2.5}$ concentrations was comparable to that of anthropogenic pollutant emissions, ranging from -6.31 to $2.32 \, \mu g \, m^{-3}$.

 CO_2 indirectly influences $PM_{2.5}$ concentrations by affecting precipitation and isoprene emissions from vegetation. In the sparsely vegetated NCP and FWP regions, CO_2 impacts near-surface $PM_{2.5}$ primarily through changes in precipitation. Conversely, in the vegetation-rich PRD region, CO_2 affects $PM_{2.5}$ concentrations mainly by altering isoprene emissions, with an impact comparable to that of anthropogenic pollutant emissions. From 2009 to 2013, the effects of anthropogenic pollutant emissions and CO_2 changes on $PM_{2.5}$ ranges are -0.25 to 3.11 and -6.19 to $-1.47\,\mu g\,m^{-3}$, respectively.

In summary, PM_{2.5} concentrations in East Asia have significantly declined since 2013, primarily driven by changes in anthropogenic pollutant emissions. During several years of the PreG period, variations in meteorological conditions affected PM_{2.5} levels to a degree comparable to that of anthropogenic pollutant emissions. However, following the implementation of the Clean Air Action Plan in 2013, the influence of anthropogenic pollutant emissions increased significantly, while the impact of meteorological factors diminished considerably. This simulation underscores the critical impor-

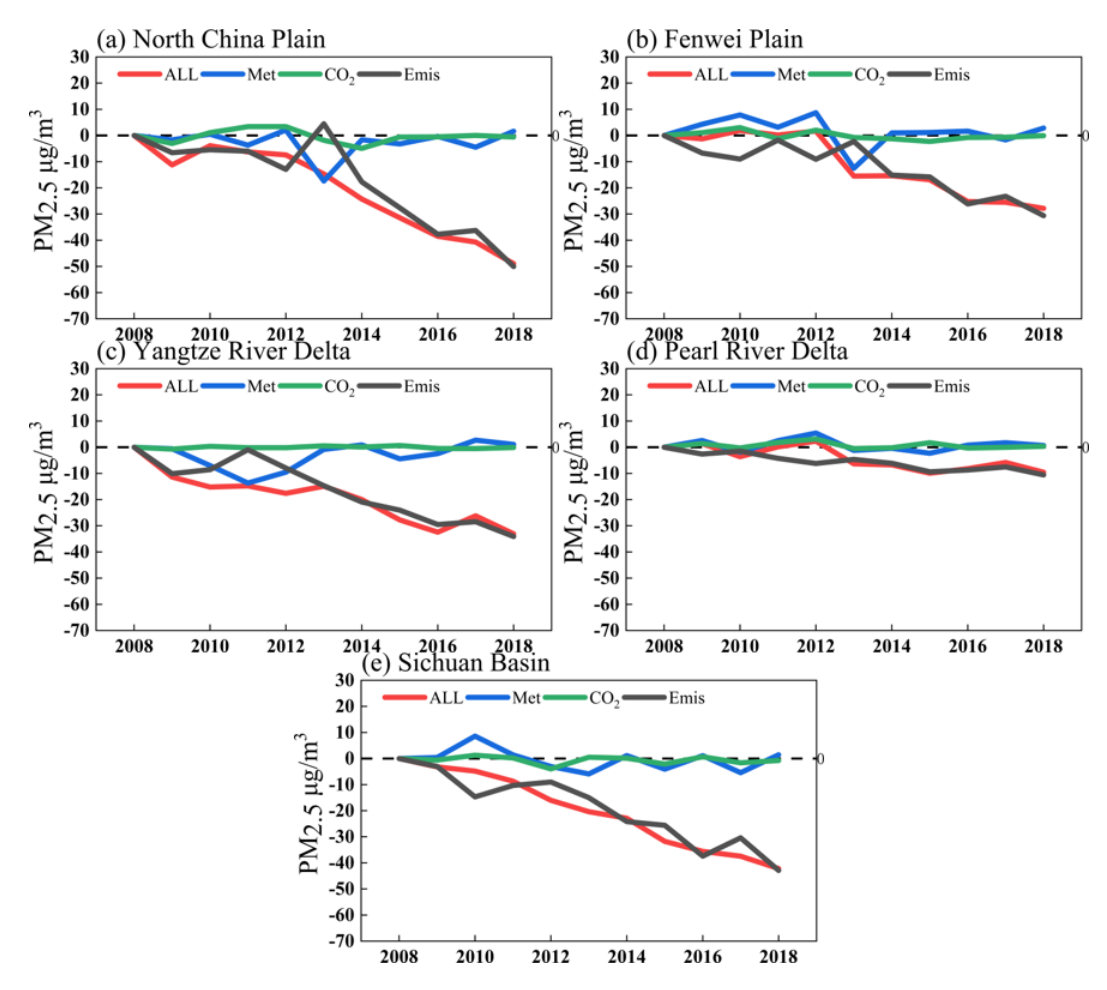


Figure 8. Changes in total $PM_{2.5}$ concentrations from 2008 to 2018 (ALL, red line) and the contributions of anthropogenic pollutant emissions (Emis, black line), meteorological conditions (Met, blue line), and CO_2 emission changes (CO_2 , green line) to $PM_{2.5}$ concentrations (Units: $\mu g m^{-3}$).

tance of stringent air pollution control measures in mitigating $PM_{2.5}$ concentrations. Moreover, we highlight that in regions with dense vegetation cover, changes in CO_2 emissions play a noteworthy role in regulating $PM_{2.5}$ levels, with the average effect during the PostG period even surpassing that of meteorological conditions. Given the sustained rise in CO_2 levels in recent years, it is imperative to integrate the modulatory effects of CO_2 into $PM_{2.5}$ simulating models and control strategies.

Data availability. ERA-Interim data available https://cds.climate.copernicus.eu/datasets/ reanalysis-era-interim?tab=d download (last access: May 2024: https://doi.org/10.24381/cds.f2f5241d; Balsamo et al., 2015). MEIC data are available at http: //meicmodel.org/?page_id=560 (last access: 20 April 2024; Zheng et al., 2018). CarbonTracker data are available at https://gml.noaa.gov/aftp/products/carbontracker/co2/CT2019/ (last access: 25 April 2024; Buchwitz et al., 2021). World Data Centre for Greenhouse Gases CO₂ data are available at https://gaw.kishou.go.jp/search/gas_species/co2/latest/ (last access: 22 April 2023; Diao et al., 2017). Data from the China National Environmental Monitoring Center are available at http://openaq.org/and https://www.cnemc.cn/en/ (Kong et al., 2021).

Supplement. The supplement related to this article is available online at https://doi.org/10.5194/acp-25-12069-2025-supplement.

Author contributions. MX, TW, and DM: designed the research, and DM: carried it out. MX, and LF: provided technical support on the RegCM-Chem-YIBs mode. SZ and SC: improved the paper. HH: improved and edited the paper.

Competing interests. The contact author has declared that none of the authors has any competing interests.

Disclaimer. Publisher's note: Copernicus Publications remains neutral with regard to jurisdictional claims made in the text, published maps, institutional affiliations, or any other geographical representation in this paper. While Copernicus Publications makes every effort to include appropriate place names, the final responsibility lies with the authors.

Acknowledgements. We hereby acknowledge the provision of anthropogenic emissions inventory support by Tsinghua University, as well as the observed datasets provided by the China National Environmental Monitoring Center. We also extend our sincere gratitude to a broad range of other institutional partners.

Financial support. This work was supported by the National Nature Science Foundation of China (grant no. 42275102), the research start-up fund for the introduction of talents from Nanjing Normal University (grant no. 184080H201B57), the National Natural Science Foundation of China – Youth Science Fund Category C (grant no. 42505177), and the Special Science and Technology Innovation Program for Carbon Peak and Carbon Neutralization of Jiangsu Province (grant no. BE2022612).

Review statement. This paper was edited by Stefania Gilardoni and reviewed by three anonymous referees.

References

- Ait-Chaalal, F., Schneider, T., Meyer, B., and Marston, J. B.: Cumulant expansions for atmospheric flows, New J. Phys., 18, 025019, https://doi.org/10.1088/1367-2630/18/2/025019, 2016.
- An, Z. S., Huang, R. J., Zhang, R. Y., Tie, X. X., Li, G. H., Cao, J. J., Zhou, W. J., Shi, Z. G., Han, Y. M., Gu, Z. L., and Ji, Y. M.: Severe haze in northern China: A synergy of anthropogenic emissions and atmospheric processes, P. Natl. Acad. Sci. USA, 116, 8657–8666, https://doi.org/10.1073/pnas.1900125116, 2019.
- Balsamo, G., Albergel, C., Beljaars, A., Boussetta, S., Brun, E., Cloke, H., Dee, D., Dutra, E., Muñoz-Sabater, J., Pappenberger, F., de Rosnay, P., Stockdale, T., and Vitart, F.: ERA-Interim/Land: a global land surface reanalysis data set, Hydrol. Earth Syst. Sci., 19, 389–407, https://doi.org/10.5194/hess-19-389-2015, 2015.
- Bleck, R. and Benjamin, S. G.: Regional Weather Prediction with a Model Combining Terrain-following and Isentropic Coordinates. Part I: Model Description, Mon. Weather Rev., 121, 1770–1785, https://doi.org/10.1175/1520-0493(1993)121<1770:Rwpwam>2.0.Co;2, 1993.
- Buchwitz, M., Reuter, M., Noël, S., Bramstedt, K., Schneising, O., Hilker, M., Fuentes Andrade, B., Bovensmann, H., Burrows, J. P., Di Noia, A., Boesch, H., Wu, L., Landgraf, J., Aben, I., Retscher, C., O'Dell, C. W., and Crisp, D.: Can a regional-scale reduction of atmospheric CO₂ during the COVID-19 pandemic be detected from space? A case study for East China using satellite XCO₂ retrievals, Atmos. Meas. Tech., 14, 2141–2166, https://doi.org/10.5194/amt-14-2141-2021, 2021.

- Cao, L., Bala, G., and Caldeira, K.: Climate response to changes in atmospheric carbon dioxide and solar irradiance on the time scale of days to weeks, Environ. Res. Lett., 7, 034015, https://doi.org/10.1088/1748-9326/7/3/034015, 2012.
- Chen, G. B., Li, S. S., Knibbs, L. D., Hamm, N. A. S., Cao, W., Li, T. T., Guo, J. P., Ren, H. Y., Abramson, M. J., and Guo, Y. M.: A machine learning method to estimate PM_{2.5} concentrations across China with remote sensing, meteorological and land use information, Sci. Total Environ., 636, 52–60, https://doi.org/10.1016/j.scitotenv.2018.04.251, 2018.
- Chen, L., Zhu, J., Liao, H., Yang, Y., and Yue, X.: Meteorological influences on PM_{2.5} and O₃ trends and associated health burden since China's clean air actions, Sci. Total Environ., 744, 140837, https://doi.org/10.1016/j.scitotenv.2020.140837, 2020a.
- Chen, Z. Y., Chen, D. L., Zhao, C. F., Kwan, M. P., Cai, J., Zhuang, Y., Zhao, B., Wang, X. Y., Chen, B., Yang, J., Li, R. Y., He, B., Gao, B. B., Wang, K. C., and Xu, B.: Influence of meteorological conditions on PM_{2.5} concentrations across China: A review of methodology and mechanism, Environ. Int., 139, 105558, https://doi.org/10.1016/j.envint.2020.105558, 2020b.
- Cheng, J., Su, J., Cui, T., Li, X., Dong, X., Sun, F., Yang, Y., Tong, D., Zheng, Y., Li, Y., Li, J., Zhang, Q., and He, K.: Dominant role of emission reduction in PM_{2.5} air quality improvement in Beijing during 2013–2017: a model-based decomposition analysis, Atmos. Chem. Phys., 19, 6125–6146, https://doi.org/10.5194/acp-19-6125-2019, 2019.
- Diao, A. Y., Shu, J., Song, C., and Gao, W.: Global consistency check of AIRS and IASI total CO₂ column concentrations using WDCGG ground-based measurements, Frontiers of Earth Science,11,1–10, https://doi.org/10.1007/s11707-016-0573-4, 2017.
- Feng, S. L., Gao, D., Liao, F., Zhou, F. R., and Wang, X. M.: The health effects of ambient PM_{2.5} and potential mechanisms, Ecotox. Environ. Safe., 128, 67–74, https://doi.org/10.1016/j.ecoenv.2016.01.030, 2016.
- Fontes, T., Li, P. L., Barros, N., and Zhao, P. J.: Trends of PM_{2.5} concentrations in China: A long term approach, J. Environ. Manage., 196, 719–732, https://doi.org/10.1016/j.jenvman.2017.03.074, 2017.
- Gao, L. B., Wang, T. J., Ren, X. J., Ma, D. Y., Zhuang, B. L., Li, S., Xie, M., Li, M. M., and Yang, X. Q.: Subseasonal characteristics and meteorological causes of surface O₃ in different East Asian summer monsoon periods over the North China Plain during 2014–2019, Atmos. Environ., 264, 118704, https://doi.org/10.1016/j.atmosenv.2021.118704, 2021.
- Geng, G. N., Liu, Y. X., Liu, Y., Liu, S. G., Cheng, J., Yan, L., Wu, N. N., Hu, H. W., Tong, D., Zheng, B., Yin, Z. C., He, K. B., and Zhang, Q.: Efficacy of China's clean air actions to tackle PM_{2.5} pollution between 2013 and 2020, Nat. Geosci., 17, 987–994, https://doi.org/10.1038/s41561-024-01540-z, 2024.
- Harris, L. M., Lin, S. J., and Tu, C. Y.: High-Resolution Climate Simulations Using GFDL HiRAM with a Stretched Global Grid, J. Climate, 29, 4293–4314, https://doi.org/10.1175/jcli-d-15-0389.1, 2016.
- Heald, C. L., Wilkinson, M. J., Monson, R. K., Alo, C. A., Wang, G. L., and Guenther, A.: Response of isoprene emission to ambient CO₂ changes and implications for global budgets, Global Change Biol., 15, 1127–1140, https://doi.org/10.1111/j.1365-2486.2008.01802.x, 2009.

- Hong, C., Zhang, Q., He, K., Guan, D., Li, M., Liu, F., and Zheng, B.: Variations of China's emission estimates: response to uncertainties in energy statistics, Atmos. Chem. Phys., 17, 1227–1239, https://doi.org/10.5194/acp-17-1227-2017, 2017.
- Hu, B., Zhao, X. J., Liu, H., Liu, Z. R., Song, T., Wang, Y. S., Tang, L. Q., Xia, X. G., Tang, G. Q., Ji, D. S., Wen, T. X., Wang, L. L., Sun, Y., and Xin, J. Y.: Quantification of the impact of aerosol on broadband solar radiation in North China, Sci. Rep.-UK, 7, 44851, https://doi.org/10.1038/srep44851, 2017.
- Huang, B. Y., Liu, C. Y., Banzon, V., Freeman, E., Graham, G., Hankins, B., Smith, T., and Zhang, H. M.: Improvements of the Daily Optimum Interpolation Sea Surface Temperature (DOISST) Version 2.1, J. Climate, 34, 2923–2939, https://doi.org/10.1175/jclid-20-0166.1, 2021.
- Kellomaki, S. and Wang, K. Y.: Growth, respiration and nitrogen content in needles of Scots pine exposed to elevated ozone and carbon dioxide in the field, Environ. Pollut., 101, 263–274, https://doi.org/10.1016/s0269-7491(98)00036-0, 1998.
- Kergoat, L., Lafont, S., Douville, H., Berthelot, B., Dedieu, G., Planton, S., and Royer, J. F.: Impact of doubled CO₂ on global-scale leaf area index and evapotranspiration: Conflicting stomatal conductance and LAI responses: art. no. 4808, J. Geophys. Res.-Atmos., 107, ACL 30-1–ACL 30-16, https://doi.org/10.1029/2001jd001245, 2002.
- Kim, K. H., Kabir, E., and Kabir, S.: A review on the human health impact of airborne particulate matter, Environ. Int., 74, 136–143, https://doi.org/10.1016/j.envint.2014.10.005, 2015.
- Kleist, E., Mentel, T. F., Andres, S., Bohne, A., Folkers, A., Kiendler-Scharr, A., Rudich, Y., Springer, M., Tillmann, R., and Wildt, J.: Irreversible impacts of heat on the emissions of monoterpenes, sesquiterpenes, phenolic BVOC and green leaf volatiles from several tree species, Biogeosciences, 9, 5111– 5123, https://doi.org/10.5194/bg-9-5111-2012, 2012.
- Kong, L., Tang, X., Zhu, J., Wang, Z., Li, J., Wu, H., Wu, Q., Chen, H., Zhu, L., Wang, W., Liu, B., Wang, Q., Chen, D., Pan, Y., Song, T., Li, F., Zheng, H., Jia, G., Lu, M., Wu, L., and Carmichael, G. R.: A 6-year-long (2013–2018) high-resolution air quality reanalysis dataset in China based on the assimilation of surface observations from CNEMC, Earth Syst. Sci. Data, 13, 529–570, https://doi.org/10.5194/essd-13-529-2021, 2021.
- Kramer, A. J., Rattanavaraha, W., Zhang, Z. F., Gold, A., Surratt, J. D., and Lin, Y. H.: Assessing the oxidative potential of isoprene-derived epoxides and secondary organic aerosol, Atmos. Environ., 130, 211–218, https://doi.org/10.1016/j.atmosenv.2015.10.018, 2016.
- Kurokawa, J. and Ohara, T.: Long-term historical trends in air pollutant emissions in Asia: Regional Emission inventory in ASia (REAS) version 3, Atmos. Chem. Phys., 20, 12761–12793, https://doi.org/10.5194/acp-20-12761-2020, 2020.
- Lei, Y., Yue, X., Liao, H., Gong, C., and Zhang, L.: Implementation of Yale Interactive terrestrial Biosphere model v1.0 into GEOS-Chem v12.0.0: a tool for biosphere—chemistry interactions, Geosci. Model Dev., 13, 1137–1153, https://doi.org/10.5194/gmd-13-1137-2020, 2020.
- Li, G., Bei, N., Cao, J., Huang, R., Wu, J., Feng, T., Wang, Y., Liu, S., Zhang, Q., Tie, X., and Molina, L. T.: A possible pathway for rapid growth of sulfate during haze days in China, Atmos. Chem. Phys., 17, 3301–3316, https://doi.org/10.5194/acp-17-3301-2017, 2017a.

- Li, J., Chen, X. S., Wang, Z. F., Du, H. Y., Yang, W. Y., Sun, Y. L., Hu, B., Li, J. J., Wang, W., Wang, T., Fu, P. Q., and Huang, H. L.: Radiative and heterogeneous chemical effects of aerosols on ozone and inorganic aerosols over East Asia, Sci. Total Environ., 622, 1327–1342, https://doi.org/10.1016/j.scitotenv.2017.12.041, 2018.
- Li, K., Jacob, D. J., Liao, H., Zhu, J., Shah, V., Shen, L., Bates, K. H., Zhang, Q., and Zhai, S. X.: A two-pollutant strategy for improving ozone and particulate air quality in China, Nat. Geosci., 12, 906, https://doi.org/10.1038/s41561-019-0464-x, 2019.
- Li, X., Feng, Y. J., Liang, H. Y., and Iop: The Impact of Meteorological Factors on PM_{2.5} Variations in Hong Kong, 8th International Conference on Environmental Science and Technology (ICEST), 12–14 June 2017, Technical University Of Madrid, Computer Science School, Madrid, Spain, WOS:000440342600003, https://doi.org/10.1088/1755-1315/78/1/012003, 2017b.
- Li, Z. and Mölders, N.: Interaction of impacts of doubling CO₂ and changing regional land-cover on evaporation, precipitation, and runoff at global and regional scales, Int. J. Climatol., 28, 1653–1679, https://doi.org/10.1002/joc.1666, 2008.
- Lin, C. Q., Liu, G., Lau, A. K. H., Li, Y., Li, C. C., Fung, J. C. H., and Lao, X. Q.: High-resolution satellite remote sensing of provincial PM_{2.5} trends in China from 2001 to 2015, Atmos. Environ., 180, 110–116, https://doi.org/10.1016/j.atmosenv.2018.02.045, 2018.
- Lin, Y.-H., Knipping, E. M., Edgerton, E. S., Shaw, S. L., and Surratt, J. D.: Investigating the influences of SO₂ and NH₃ levels on isoprene-derived secondary organic aerosol formation using conditional sampling approaches, Atmos. Chem. Phys., 13, 8457–8470, https://doi.org/10.5194/acp-13-8457-2013, 2013.
- Lindwall, F., Schollert, M., Michelsen, A., Blok, D., and Rinnan, R.: Fourfold higher tundra volatile emissions due to arctic summer warming, J. Geophys. Res.-Biogeo., 121, 895–902, https://doi.org/10.1002/2015jg003295, 2016.
- Ma, D., Wang, T., Wu, H., Qu, Y., Liu, J., Liu, J., Li, S., Zhuang, B., Li, M., and Xie, M.: The effect of anthropogenic emission, meteorological factors, and carbon dioxide on the surface ozone increase in China from 2008 to 2018 during the East Asia summer monsoon season, Atmos. Chem. Phys., 23, 6525–6544, https://doi.org/10.5194/acp-23-6525-2023, 2023a.
- Ma, D. Y., Wang, T. J., Xu, B. Y., Song, R., Gao, L. B., Chen, H. M., Ren, X. J., Li, S., Zhuang, B. L., Li, M. M., Xie, M., and Saikawa, E.: The mutual interactions among ozone, fine particulate matter, and carbon dioxide on summer monsoon climate in East Asia, Atmos. Environ., 299, 119668, https://doi.org/10.1016/j.atmosenv.2023.119668, 2023b.
- Ma, Z., Liu, R., Liu, Y., and Bi, J.: Effects of air pollution control policies on PM_{2.5} pollution improvement in China from 2005 to 2017: a satellite-based perspective, Atmos. Chem. Phys., 19, 6861–6877, https://doi.org/10.5194/acp-19-6861-2019, 2019.
- Ma, Z. W., Hu, X. F., Sayer, A. M., Levy, R., Zhang, Q., Xue, Y. G., Tong, S. L., Bi, J., Huang, L., and Liu, Y.: Satellite-Based Spatiotemporal Trends in PM_{2.5} Concentrations: China, 2004–2013, Environ. Health Persp., 124, 184–192, https://doi.org/10.1289/ehp.1409481, 2016.
- Matthews, H. D.: Implications of CO₂ fertilization for future climate change in a coupled climate-carbon model, Global Change Biol., 13, 1068–1078, https://doi.org/10.1111/j.1365-2486.2007.01343.x, 2007.

- Mousavinezhad, S., Choi, Y., Pouyaei, A., Ghahremanloo, M., and Nelson, D. L.: A comprehensive investigation of surface ozone pollution in China, 2015–2019: Separating the contributions from meteorology and precursor emissions, Atmos. Res., 257, 105599, https://doi.org/10.1016/j.atmosres.2021.105599, 2021.
- Pan, L., Xu, J. M., Tie, X. X., Mao, X. Q., Gao, W., and Chang, L. Y.: Long-term measurements of planetary boundary layer height and interactions with PM_{2.5} in Shanghai, China, Atmos. Pollut. Res., 10, 989–996, https://doi.org/10.1016/j.apr.2019.01.007, 2019.
- Pegoraro, E., Rey, A., Bobich, E. G., Barron-Gafford, G., Grieve, K. A., Malhi, Y., and Murthy, R.: Effect of elevated CO₂ concentration and vapour pressure deficit on isoprene emission from leaves of *Populus deltoides* during drought, Funct. Plant Biol., 31, 1137–1147, https://doi.org/10.1071/fp04142, 2004.
- Peters, W., Jacobson, A. R., Sweeney, C., Andrews, A. E., Conway, T. J., Masarie, K., Miller, J. B., Bruhwiler, L. M. P., Petron, G., Hirsch, A. I., Worthy, D. E. J., van der Werf, G. R., Randerson, J. T., Wennberg, P. O., Krol, M. C., and Tans, P. P.: An atmospheric perspective on North American carbon dioxide exchange: CarbonTracker, P. Natl. Acad. Sci. USA, 104, 18925–18930, https://doi.org/10.1073/pnas.0708986104, 2007.
- Possell, M., Hewitt, C. N., and Beerling, D. J.: The effects of glacial atmospheric CO₂ concentrations and climate on isoprene emissions by vascular plants, Global Change Biol., 11, 60–69, https://doi.org/10.1111/j.1365-2486.2004.00889.x, 2005.
- Pui, D. Y. H., Chen, S. C., and Zuo, Z. L.: PM_{2.5} in China: Measurements, sources, visibility and health effects, and mitigation, Particuology, 13, 1–26, https://doi.org/10.1016/j.partic.2013.11.001, 2014.
- Ringler, T., Petersen, M., Higdon, R. L., Jacobsen, D., Jones, P. W., and Maltrud, M.: A multi-resolution approach to global ocean modeling, Ocean Model., 69, 211–232, https://doi.org/10.1016/j.ocemod.2013.04.010, 2013.
- Shalaby, A., Zakey, A. S., Tawfik, A. B., Solmon, F., Giorgi, F., Stordal, F., Sillman, S., Zaveri, R. A., and Steiner, A. L.: Implementation and evaluation of online gas-phase chemistry within a regional climate model (RegCM-CHEM4), Geosci. Model Dev., 5, 741–760, https://doi.org/10.5194/gmd-5-741-2012, 2012.
- Silver, B., Reddington, C. L., Arnold, S. R., and Spracklen, D. V.: Substantial changes in air pollution across China during 2015–2017, Environ. Res. Lett., 13, 114012, https://doi.org/10.1088/1748-9326/aae718, 2018.
- Silver, B., Reddington, C. L., Chen, Y., and Arnold, S. R.: A decade of China's air quality monitoring data suggests health impacts are no longer declining, Environ. Int., 197, 109318, https://doi.org/10.1016/j.envint.2025.109318, 2025.
- Sun, Z. H., Niinemets, Ü., Hüve, K., Noe, S. M., Rasulov, B., Copolovici, L., and Vislap, V.: Enhanced isoprene emission capacity and altered light responsiveness in aspen grown under elevated atmospheric CO₂ concentration, Global Change Biol., 18, 3423–3440, https://doi.org/10.1111/j.1365-2486.2012.02789.x, 2012.
- Sun, Z. H., Hve, K., Vislap, V., and Niinemets, U.: Elevated CO₂ magnifies isoprene emissions under heat and improves thermal resistance in hybrid aspen, J. Exp. Bot., 64, 5509–5523, https://doi.org/10.1093/jxb/ert318, 2013.
- van Donkelaar, A., Martin, R. V., Brauer, M., Kahn, R., Levy, R., Verduzco, C., and Villeneuve, P. J.: Global Es-

- timates of Ambient Fine Particulate Matter Concentrations from Satellite-Based Aerosol Optical Depth: Development and Application, Environ. Health Persp., 118, 847–855, https://doi.org/10.1289/ehp.0901623, 2010.
- van Donkelaar, A., Martin, R. V., Li, C., and Burnett, R. T.: Regional Estimates of Chemical Composition of Fine Particulate Matter Using a Combined Geoscience-Statistical Method with Information from Satellites, Models, and Monitors, Environ. Sci. Technol., 53, 2595–2611, https://doi.org/10.1021/acs.est.8b06392, 2019.
- Vu, T. V., Shi, Z., Cheng, J., Zhang, Q., He, K., Wang, S., and Harrison, R. M.: Assessing the impact of clean air action on air quality trends in Beijing using a machine learning technique, Atmos. Chem. Phys., 19, 11303–11314, https://doi.org/10.5194/acp-19-11303-2019, 2019.
- Wang, H., Peng, Y., Zhang, X., Liu, H., Zhang, M., Che, H., Cheng, Y., and Zheng, Y.: Contributions to the explosive growth of PM_{2.5} mass due to aerosol–radiation feedback and decrease in turbulent diffusion during a red alert heavy haze in Beijing–Tianjin–Hebei, China, Atmos. Chem. Phys., 18, 17717–17733, https://doi.org/10.5194/acp-18-17717-2018, 2018a.
- Wang, H., Tian, M., Chen, Y., Shi, G., Liu, Y., Yang, F., Zhang, L., Deng, L., Yu, J., Peng, C., and Cao, X.: Seasonal characteristics, formation mechanisms and source origins of PM_{2.5} in two megacities in Sichuan Basin, China, Atmos. Chem. Phys., 18, 865–881, https://doi.org/10.5194/acp-18-865-2018, 2018b.
- Wang, J. D., Zhao, B., Wang, S. X., Yang, F. M., Xing, J., Morawska, L., Ding, A. J., Kulmala, M., Kerminen, V. M., Kujansuu, J., Wang, Z. F., Ding, D. A., Zhang, X. Y., Wang, H. B., Tian, M., Petaja, T., Jiang, J. K., and Hao, J. M.: Particulate matter pollution over China and the effects of control policies, Sci. Total Environ., 584, 426–447, https://doi.org/10.1016/j.scitotenv.2017.01.027, 2017.
- Wei, J., Li, Z. Q., Lyapustin, A., Sun, L., Peng, Y. R., Xue, W. H., Su, T. N., and Cribb, M.: Reconstructing 1-km-resolution high-quality PM_{2.5} data records from 2000 to 2018 in China: spatiotemporal variations and policy implications, Remote Sens. Environ., 252, 112136, 10.1016/j.rse.2020.112136, 2021.
- Wilkinson, M. J., Monson, R. K., Trahan, N., Lee, S., Brown, E., Jackson, R. B., Polley, H. W., Fay, P. A., and Fall, R.: Leaf isoprene emission rate as a function of atmospheric CO₂ concentration, Global Change Biol., 15, 1189–1200, https://doi.org/10.1111/j.1365-2486.2008.01803.x, 2009.
- Wu, H., Wang, T. J., Wang, Q., Cao, Y., Qu, Y. W., and Nie, D. Y.: Radiative effects and chemical compositions of fine particles modulating urban heat island in Nanjing, China, Atmos. Environ., 247, 118201, https://doi.org/10.1016/j.atmosenv.2021.118201, 2021.
- Wu, K., Yang, X. Y., Chen, D., Gu, S., Lu, Y. Q., Jiang, Q., Wang, K., Ou, Y. H., Qian, Y., Shao, P., and Lu, S. H.: Estimation of biogenic VOC emissions and their corresponding impact on ozone and secondary organic aerosol formation in China, Atmos. Res., 231, 104656, https://doi.org/10.1016/j.atmosres.2019.104656, 2020.
- Wu, Y. N., Liu, J. K., Zhai, J. X., Cong, L., Wang, Y., Ma, W. M., Zhang, Z. M., and Li, C. Y.: Comparison of dry and wet deposition of particulate matter in nearsurface waters during summer, Plos One, 13, e0199241, https://doi.org/10.1371/journal.pone.0199241, 2018.

- Xiao, Q., Zheng, Y., Geng, G., Chen, C., Huang, X., Che, H., Zhang, X., He, K., and Zhang, Q.: Separating emission and meteorological contributions to long-term PM_{2.5} trends over eastern China during 2000–2018, Atmos. Chem. Phys., 21, 9475–9496, https://doi.org/10.5194/acp-21-9475-2021, 2021.
- Xie, N., Wang, T., Xie, X., Yue, X., Giorgi, F., Zhang, Q., Ma, D., Song, R., Xu, B., Li, S., Zhuang, B., Li, M., Xie, M., Andreeva Kilifarska, N., Gadzhev, G., and Dimitrova, R.: The regional climate–chemistry–ecology coupling model RegCM-Chem (v4.6)–YIBs (v1.0): development and application, Geosci. Model Dev., 17, 3259–3277, https://doi.org/10.5194/gmd-17-3259-2024, 2024.
- Xie, X., Wang, T., Yue, X., Li, S., Zhuang, B., Wang, M., and Yang, X.: Numerical modeling of ozone damage to plants and its effects on atmospheric CO₂ in China, Atmos. Environ., 217, 116970, https://doi.org/10.1016/j.atmosenv.2019.116970, 2019.
- Xing, Y. F., Xu, Y. H., Shi, M. H., and Lian, Y. X.: The impact of PM_{2.5} on the human respiratory system, J. Thorac. Dis., 8, E69– E74, https://doi.org/10.3978/j.issn.2072-1439.2016.01.19, 2016.
- Xu, B. Y., Wang, T. J., Ma, D. Y., Song, R., Zhang, M., Gao, L. B., Li, S., Zhuang, B. L., Li, M. M., and Xie, M.: Impacts of regional emission reduction and global climate change on air quality and temperature to attain carbon neutrality in China, Atmos. Res., 279, 106384, https://doi.org/10.1016/j.atmosres.2022.106384, 2022.
- Xu, B. Y., Wang, T. J., Gao, L. B., Ma, D. Y., Song, R., Zhao, J., Yang, X. G., Li, S., Zhuang, B. L., Li, M. M., and Xie, M.: Impacts of meteorological factors and ozone variation on crop yields in China concerning carbon neutrality objectives in 2060, Environ. Pollut., 317, 120715, https://doi.org/10.1016/j.envpol.2022.120715, 2023.
- Xue, W. H., Zhang, J., Zhong, C., Ji, D. Y., and Huang, W.: Satellite-derived spatiotemporal PM_{2.5} concentrations and variations from 2006 to 2017 in China, Sci. Total Environ., 712, 134577, https://doi.org/10.1016/j.scitotenv.2019.134577, 2020.
- Yue, X. and Unger, N.: The Yale Interactive terrestrial Biosphere model version 1.0: description, evaluation and implementation into NASA GISS ModelE2, Geosci. Model Dev., 8, 2399–2417, https://doi.org/10.5194/gmd-8-2399-2015, 2015.
- Yue, X., Unger, N., and Zheng, Y.: Distinguishing the drivers of trends in land carbon fluxes and plant volatile emissions over the past 3 decades, Atmos. Chem. Phys., 15, 11931–11948, https://doi.org/10.5194/acp-15-11931-2015, 2015.
- Zhai, S., Jacob, D. J., Wang, X., Shen, L., Li, K., Zhang, Y., Gui, K., Zhao, T., and Liao, H.: Fine particulate matter (PM_{2.5}) trends in China, 2013–2018: separating contributions from anthropogenic emissions and meteorology, Atmos. Chem. Phys., 19, 11031–11041, https://doi.org/10.5194/acp-19-11031-2019, 2019.

- Zhang, B. E., Jiao, L. M., Xu, G., Zhao, S. L., Tang, X., Zhou, Y., and Gong, C.: Influences of wind and precipitation on different-sized particulate matter concentrations ($PM_{2.5}$, PM_{10} , $PM_{2.5-10}$), Meteorol. Atmos. Phys., 130, 383–392, https://doi.org/10.1007/s00703-017-0526-9, 2018.
- Zhang, Q., Zheng, Y. X., Tong, D., Shao, M., Wang, S. X., Zhang, Y. H., Xu, X. D., Wang, J. N., He, H., Liu, W. Q., Ding, Y. H., Lei, Y., Li, J. H., Wang, Z. F., Zhang, X. Y., Wang, Y. S., Cheng, J., Liu, Y., Shi, Q. R., Yan, L., Geng, G. N., Hong, C. P., Li, M., Liu, F., Zheng, B., Cao, J. J., Ding, A. J., Gao, J., Fu, Q. Y., Huo, J. T., Liu, B. X., Liu, Z. R., Yang, F. M., He, K. B., and Hao, J. M.: Drivers of improved PM_{2.5} air quality in China from 2013 to 2017, P. Natl. Acad. Sci. USA, 116, 24463–24469, https://doi.org/10.1073/pnas.1907956116, 2019.
- Zhang, Y., Olsen, K. M., and Wang, K.: Fine Scale Modeling of Agricultural Air Quality over the Southeastern United States Using Two Air Quality Models. Part I. Application and Evaluation, Aerosol Air Qual. Res., 13, 1231–1252, https://doi.org/10.4209/aaqr.2012.12.0346, 2013.
- Zhang, Y., Gentine, P., Luo, X. Z., Lian, X., Liu, Y. L., Zhou, S., Michalak, A. M., Sun, W., Fisher, J. B., Piao, S. L., and Keenan, T. F.: Increasing sensitivity of dryland vegetation greenness to precipitation due to rising atmospheric CO₂, Nat. Commun., 13, 4875, https://doi.org/10.1038/s41467-022-32631-3, 2022.
- Zheng, B., Tong, D., Li, M., Liu, F., Hong, C., Geng, G., Li, H., Li, X., Peng, L., Qi, J., Yan, L., Zhang, Y., Zhao, H., Zheng, Y., He, K., and Zhang, Q.: Trends in China's anthropogenic emissions since 2010 as the consequence of clean air actions, Atmos. Chem. Phys., 18, 14095–14111, https://doi.org/10.5194/acp-18-14095-2018, 2018.
- Zheng, B., Cheng, J., Geng, G. N., Wang, X., Li, M., Shi, Q. R., Qi, J., Lei, Y., Zhang, Q., and He, K. B.: Mapping anthropogenic emissions in China at 1 km spatial resolution and its application in air quality modeling, Sci. Bull., 66, 612–620, https://doi.org/10.1016/j.scib.2020.12.008, 2021a.
- Zheng, B., Zhang, Q., Geng, G., Chen, C., Shi, Q., Cui, M., Lei, Y., and He, K.: Changes in China's anthropogenic emissions and air quality during the COVID-19 pandemic in 2020, Earth Syst. Sci. Data, 13, 2895–2907, https://doi.org/10.5194/essd-13-2895-2021, 2021b.
- Zhong, J., Zhang, X., Dong, Y., Wang, Y., Liu, C., Wang, J., Zhang, Y., and Che, H.: Feedback effects of boundary-layer meteorological factors on cumulative explosive growth of PM_{2.5} during winter heavy pollution episodes in Beijing from 2013 to 2016, Atmos. Chem. Phys., 18, 247–258, https://doi.org/10.5194/acp-18-247-2018, 2018.